



HAL
open science

Hydrological Signals in Height and Gravity in Northeastern Italy inferred from Principal Components Analysis

S. Zerbini, F. Raicich, B. Richter, V. Gorini, M. Errico

► **To cite this version:**

S. Zerbini, F. Raicich, B. Richter, V. Gorini, M. Errico. Hydrological Signals in Height and Gravity in Northeastern Italy inferred from Principal Components Analysis. *Journal of Geodynamics*, 2010, 49 (3-4), pp.190. 10.1016/j.jog.2009.11.001 . hal-00615315

HAL Id: hal-00615315

<https://hal.science/hal-00615315>

Submitted on 19 Aug 2011

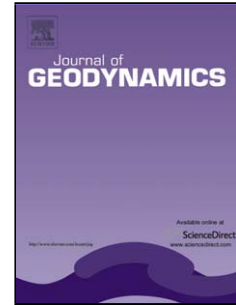
HAL is a multi-disciplinary open access archive for the deposit and dissemination of scientific research documents, whether they are published or not. The documents may come from teaching and research institutions in France or abroad, or from public or private research centers.

L'archive ouverte pluridisciplinaire **HAL**, est destinée au dépôt et à la diffusion de documents scientifiques de niveau recherche, publiés ou non, émanant des établissements d'enseignement et de recherche français ou étrangers, des laboratoires publics ou privés.

Accepted Manuscript

Title: Hydrological Signals in Height and Gravity in Northeastern Italy inferred from Principal Components Analysis

Authors: S. Zerbini, F. Raicich, B. Richter, V. Gorini, M. Errico



PII: S0264-3707(09)00152-5
DOI: doi:10.1016/j.jog.2009.11.001
Reference: GEOD 950

To appear in: *Journal of Geodynamics*

Received date: 23-1-2009
Revised date: 28-10-2009
Accepted date: 10-11-2009

Please cite this article as: Zerbini, S., Raicich, F., Richter, B., Gorini, V., Errico, M., Hydrological Signals in Height and Gravity in Northeastern Italy inferred from Principal Components Analysis, *Journal of Geodynamics* (2008), doi:10.1016/j.jog.2009.11.001

This is a PDF file of an unedited manuscript that has been accepted for publication. As a service to our customers we are providing this early version of the manuscript. The manuscript will undergo copyediting, typesetting, and review of the resulting proof before it is published in its final form. Please note that during the production process errors may be discovered which could affect the content, and all legal disclaimers that apply to the journal pertain.

Hydrological Signals in Height and Gravity in Northeastern Italy inferred from Principal Components Analysis

S. Zerbini^{a,*}, F. Raicich^b, B. Richter^c, V. Gorini^a, M. Errico^a

^a *Dipartimento di Fisica, Università di Bologna, Viale Berti Pichat 8, I-40127 Bologna, Italy*

^b *CNR-Istituto di Scienze Marine, Sede di Trieste, V.le Romolo Gessi 2, I-34123, Trieste, Italy*

^c *Bundesamt fuer Kartographie und Geodaesie, Richard-Strauss-Allee 11, D-60598 Frankfurt am
Main, Germany*

Abstract

This work describes a study of GPS heights, gravity and hydrological time series collected by stations located in northeastern Italy. During the last 12 years, changes in the long-term behaviors of the GPS heights and gravity time series are observed. In particular, starting in 2004-2005, a height increase is observed over the whole area. The temporal and spatial variability of these parameters has been studied as well as those of key hydrological variables, namely precipitation, hydrological balance and water table by using the Empirical Orthogonal Functions (EOF) analysis. The coupled variability between the GPS heights and the hydrological balance and precipitation data has been investigated by means of the Singular Value Decomposition (SVD) approach. Significant common patterns in the spatial and temporal variability of these parameters have been recognized. In particular, hydrology-induced variations are clearly observable starting in 2002-2003 in the southern part of the Po Plain for the longest time series, and from 2004-2005 over the whole area. These findings, obtained by means of purely mathematical approaches, are supported by sound physical interpretation suggesting that the climate-related fluctuations in the regional/local hydrological regime are one of the main

* Corresponding author.

E-mail address: susanna.zerbini@unibo.it

29 contributors to the observed variations. A regional scale signal has been identified in the
30 GPS station heights; it is characterized by the opposite behavior of the southern and
31 northern stations in response to the hydrological forcing. At Medicina, in the southern Po
32 Plain, the EOF analysis has shown a marked common signal between the GPS heights
33 and the Superconducting Gravimeter (SG) data both over the long and the short period.

34

35 *Keywords:* GPS height; gravity; hydrology; subsidence; Empirical Orthogonal Functions;
36 Singular Value Decomposition method

37

38 **1.0 Introduction**

39

40 The long (multi year) and short (seasonal to a few years) period oscillations
41 observed in the continuous time series of GPS heights and gravity result from the
42 superimposition of various phenomena of different physical nature. Among them,
43 tectonics and the mass transport in the Earth's system which induces deformation of the
44 Earth's crust in response to variations of the load due to hydrology, air pressure and non-
45 tidal oceanic effects. Continuous GPS time series exceeding a decade are now available
46 which can provide reliable information on the long-term height evolution (linear and non-
47 linear) as well as on the short-period seasonal fluctuations. However, it is complicated to
48 unravel the contribution of the different components in the observed long-term height
49 behavior because, at global scale, the Glacial Isostatic Adjustment (GIA) is the only
50 coherent geological contribution to height variation for which understanding of the
51 physical process has been achieved. Superconducting gravimeter and/or absolute gravity

52 measurements are not as widely spread as those of GPS, but where both types of
53 measurements are available, they offer a unique means to detect and understand mass
54 contributions.

55 It was shown that hydrological mass variations play a major role in the seasonal
56 height and gravity variability (van Dam et al., 2001; Zerbini et al., 2007). On long-time
57 scales, climate-related variations of GPS heights and gravity have not yet been clearly
58 identified mainly because of the limited temporal extent of most of the continuous series
59 and for the lack of information on the spatial and temporal variability of groundwater
60 storage.

61 We have studied the variations observed during the last decade in the GPS heights,
62 gravity and the hydrological time series in northeastern Italy (Fig. 1), as well as their
63 mutual relationships. The investigated area is affected by both natural and human-
64 induced subsidence. The Po Plain is a subsiding sedimentary basin encompassed by the
65 Alps, Apennines and Dinarides Chains. Two structural environments occur within the
66 basin: the north-verging Apennine fold-and-thrust belt system that is buried under the
67 Plio-Quaternary cover and a platform gently dipping from the Alps into the basin
68 (Carminati and Martinelli, 2002). Sedimentation has filled the basin with alternate
69 stratigraphic sequences of sands, silts and clays variably interbedded and normally
70 consolidated and containing water in the form of impregnating water and groundwater
71 (Zerbini et al., 2000; 2002). These conditions are most favorable for the development of
72 both natural and anthropogenic subsidence. Long-term natural subsidence rates range
73 between 1-to-2 mm/yr (Pignone et al., 2008), with maximum rates of 2.5 mm/yr
74 evaluated from the analysis of borehole stratigraphies and from available seismic sections

75 (Carminati et al., 2003) with the largest rates occurring in the southern part of the Po
76 Plain and in the Po Delta. As discussed by Carminati and Di Donato (1999),
77 backstripping analysis suggests that tectonics accounts for about 50% of the long-term
78 natural subsidence, whereas compaction and sediment load account for about 30 and
79 20%, respectively. However, the present-day geodetic observations show subsidence
80 rates with peaks up to 40 mm/yr resulting from an anthropogenic component
81 superimposed to the natural subsidence. The anthropogenic contribution has been
82 generated by systematic exploitation of groundwater for both industrial and civil use for
83 about 50 years starting during 1950s. Groundwater control policies have been adopted
84 since the beginning of the 1980s with the consequent reduction of fluids withdrawal.

85 In our study, we have adopted the Empirical Orthogonal Functions (EOF) and the
86 Singular Value Decomposition (SVD) analyses. Significant common patterns in the
87 spatial and temporal variability of GPS heights, gravity and hydrological parameters have
88 been identified. In particular, hydrology-induced variations are clearly observable starting
89 in 2002-2003 in the southern part of the Po Plain for the longest GPS time series as well
90 as for gravity, and from 2005 for the GPS heights over the whole area. Observing and
91 modeling long- and short-period signals in the height and gravity time series allows to
92 better understand and quantify subsidence. This knowledge is important because of the
93 relevant societal impacts of this phenomenon.

94

95 **2.0 Data**

96

97 In northeastern Italy, several data sets are available that can be used for a
98 spatial/temporal analysis of potentially common signals. These are time series of GPS
99 heights, hydrological information, such as precipitation, simplified hydrological balance
100 (precipitation minus evapotranspiration) and water table data, and series of absolute
101 gravity and superconducting gravimeter measurements. Four of the GPS time series are
102 rather long (about a decade or longer) and continuous.

103

104 **2.1 GPS**

105

106 We have used the continuous GPS data of a network located in northeastern Italy
107 (Fig. 1 and Table 1). The observations were analyzed by means of the Bernese software
108 package version 5.0 (Dach et al., 2007). The data were processed by using high-accuracy
109 International GNSS Service (IGS) products including the ionospheric files, the satellite
110 orbits and the Earth rotation parameters. The ITRF2005 coordinates and velocity field
111 (Altamimi et al., 2007) were adopted for five IGS stations in Europe (ZIMM, GRAZ,
112 MEDI, MATE and CAGL) used as fiducial sites in the network adjustment procedure. In
113 Medicina, there are two GPS receivers, MEDI and MSEL, installed at a distance of about
114 30 m from each other. Both MEDI and MSEL are EUREF EPN stations. One important
115 aspect is that the antennas/receivers of the stations, except for MEDI, were never
116 substituted during the time period of the present analysis. This ensures a desirable
117 homogeneity of the height series and the absence of jumps due to a change of
118 instrumentation. The MEDI height time series presented in this paper for comparison
119 purposes is a EUREF solution kindly provided by K. Szafranek and A. Kenyeres (2009).

120

121 **2.2 Hydrology**

122

123 For all stations, we have estimated a simplified daily hydrological balance. The data
124 used were the daily precipitation and maximum and minimum air temperature to derive
125 estimates of the potential evapotranspiration according to the Hargreaves equation
126 (Hargreaves and Samani, 1982, 1985). In addition, at Medicina, continuous
127 measurements of the surficial water table are available.

128 In order to compare the hydrological balance data with those of GPS heights and
129 gravity, we have built hydrological time series in which the n-th element is the time
130 integral of the daily values from 1 (first epoch) to n. The linear trends have been removed
131 from these time series in order to highlight the seasonal to interannual variability of the
132 local hydrology. The residuals turn out to be useful proxies for the surficial water table
133 fluctuations. Precipitation, treated in the same way as the hydrological balance, also
134 appears to be a good proxy for the multi-year behavior of the water table. The
135 identification of reliable proxies is necessary because water table data are not, in general,
136 readily available. Figure 2 illustrates, as an example for the Medicina station, a
137 comparison between hydrological balance, precipitation and water table data residuals.
138 The three series are in good agreement as regards the long-term behavior and the phase of
139 the seasonal cycle. However, the amplitude of the oscillations of the water table is not
140 always well represented by the hydrological balance and precipitation.

141

142 **2.3 Gravity**

143

144 Superconducting gravimeter (SG) and absolute gravity (AG) observations are
145 performed at Medicina, while in Loiano, Bologna, Voltabarozzo, Marghera, Cavallino
146 and Treviso only AG measurements are carried out (Table 1). The continuous SG
147 measurements at Medicina start at the beginning of 1998. An instrumental linear drift
148 ($18.6 \text{ nms}^{-2}/\text{yr}$) was estimated by comparison with a series of AG measurements
149 performed by means of FG-5 instruments. The gravity data have been analyzed according
150 to the description given in Zerbini et al. (2007).

151

152 **3.0 Methods: EOF and SVD analyses**

153

154 Our objective is twofold: we aim at recognizing both spatial and temporal variability
155 patterns. We will study the behaviour of individual variables, namely GPS height,
156 gravity, precipitation, hydrological balance and water table and of variable pairs, for
157 example, GPS height and precipitation. The analysis is performed using a principal
158 component approach.

159 In particular, following the terminology proposed by Björnsson and Venegas (1997)
160 and Venegas (2001), the EOF method is used to analyse individual variables and the
161 SVD method for variable pairs. It should be mentioned that the terminology is not
162 univocal in the literature. The EOF and SVD techniques are widely used in geophysics to
163 analyse temporally and spatially varying fields allowing transforming the data into a
164 different set with some desirable properties (for more details, see Bretherton et al. (1992),

165 von Storch and Navarra (1999), Björnsson and Venegas (1997), Venegas (2001) and
166 Hannachi (2004)).

167 The variability of geophysical fields is the result of complex nonlinear interactions
168 between very many degrees of freedom, and a challenging task is to discriminate between
169 signal and noise. The definition of signal and noise depends on the specific object of
170 interest, but, in general, the signal can be a pattern in space and/or time, while the noise,
171 physical or instrumental, consists of features that are not relevant for the signal.
172 Normally, the signal has larger temporal and spatial scales and fewer degrees of freedom
173 than the noise.

174 The EOF analysis provides a compact description of the temporal and spatial
175 variability of a data set of a single variable in terms of orthogonal components or, also
176 called, statistical “modes”. Conceptually, the decomposition in EOFs is analogous to,
177 e.g., those in Fourier periodic functions or Legendre polynomials. The difference is that
178 the EOF basis functions are not analytic but empirical; the members are not chosen on
179 analytical considerations, but on maximization of the data projection on them. The first
180 EOF is selected to be the pattern on which the data project most strongly. In other words,
181 the leading EOF is the pattern most frequently realized. The second mode is the one most
182 commonly realized under the constraint of orthogonality to the first one, the third is the
183 most frequently realized pattern that is orthogonal to both higher modes, and so on.

184 Each EOF is associated to a percentage of the total variance (PVE, percent variance
185 explained) of the original data set, which accounts for the relative importance of the
186 corresponding mode of variability. This allows recognizing dominant modes, which are
187 likely to compose the signal, leaving out the remainder, which is the noise.

188 Let $f(x,t)$ be the variable of interest, defined at n locations (x_1, \dots, x_n) and at m times
 189 (t_1, \dots, t_m) . The data are usually arranged in a $m \times n$ matrix (F), where each of the n columns
 190 represents the time series for a given location, and each of the m rows represents the
 191 spatial distribution at a given time. F can be written as:

192

193

$$F = U\Gamma V^T$$

194

195 Γ is a rectangular ($m \times n$) matrix with positive or zero elements on the diagonal (γ_k ,
 196 $k=1, \dots, \min(m,n)$) and zeroes elsewhere. U is a ($m \times m$) quadratic matrix, whose
 197 columns (u^k) are orthogonal and represent the EOFs, (or modes or patterns, functions of
 198 space only). V^T is a ($n \times n$) quadratic matrix, whose rows (v^{Tk}) are also orthogonal and
 199 represent the principal components (functions of time only).

200 The original field can be reconstructed as a linear combination of all the modes:

201

$$F_m(t) = \sum_k u_m^k a_k(t)$$

202

203 where $a_k(t) = \gamma_k v^{Tk}(t)$. Since, in the literature, the nomenclature of the quantities involved
 204 in the analysis is not univocal, we will call u^k the “spatial patterns” and a_k the “time
 205 components”.

206

207

208

The SVD technique has the same purpose as the EOF, but each component describes
 a mode of coupled variability of two fields. Similarly to the EOF, each SVD is associated
 to a percentage of total covariance (SCP, squared covariance percentage).

209

210

The strength of the coupling for each SVD can be quantified by estimating the
 correlation coefficient between the relevant time components. In order to assess the

211 confidence level of such correlation, we need the number of independent data pairs (N_{ind})
212 involved (i.e. the number of degrees of freedom). In our case, a rigorous estimate is
213 difficult, therefore we adopt the following definition: $N_{ind} = N_{tot}T_d / T$. Here N_{tot} is the
214 number of available data pairs, T_d the “decorrelation time”, namely the first zero of the
215 time autocovariance function of the involved variables, and T the length of the time
216 interval covered by all the data. In the present analysis, the GPS data exhibit quite larger
217 T_d values (1.2-1.3 years) than the hydrological balance does (about 0.4 years) and
218 precipitation (about 0.5 years). As a consequence, the number of independent data pairs is
219 approximately reduced by a factor of 20, when the hydrological balance is involved, or
220 by a factor of 30, in the case of precipitation.

221 It shall be pointed out that these analyses are purely statistical; therefore the
222 physical interpretation of the individual components requires specific arguments.

223

224 **4.0 Linear trends: GPS height, gravity and hydrology**

225

226 All stations, except Loiano, which is on the uprising chain of the Apennines, are
227 located in the Po Plain and northeastern Adriatic; this area is characterized by relevant
228 natural subsidence. The largest rates are mainly of anthropogenic nature (Zerbini et al.,
229 2007). Figure 3 presents the time series of the GPS heights in the ITRF2005 and the AG
230 and SG gravity series of the stations in the network. Gravity has been multiplied by a
231 factor (-1) in order to facilitate the visual comparison with the height data. The height
232 time series show a decrease in the subsidence rates starting around 2004-2005; an
233 exception is San Felice which, instead, exhibits an increase in subsidence. Table 1 lists,

234 both for GPS and gravity, the linear trends computed over the entire time span. The
235 formal errors associated to the linear trend estimates both of GPS height and gravity have
236 been multiplied by an arbitrary factor of 5 in order to provide a conservative estimate of
237 the errors. Figure 3d concerns the Medicina station. It presents the MEDI and MSEL GPS
238 height series as well as the SG and AG gravity observations multiplied by (-1). The two
239 GPS series and those of gravity are comparable. They all show from about 2005 a
240 different long-term behavior, a reduction of subsidence, with even a tendency to uplift
241 during the last two years 2006-2007.

242 In Bologna (EUREF EPN station BOLG, Figure 3c), the linear trend turns out to be
243 -10.57 ± 0.25 mm/yr for the period 1999-2008 and -8.31 ± 0.40 mm/yr in the time frame
244 2002-2008 corresponding to the period for which absolute gravity measurements are also
245 available. The trend estimated from the gravity data is $+4.17 \pm 1.75$ μ Gal/yr, consistent
246 with the GPS results, within the statistical error, if using the free-air conversion factor
247 (Vaníček and Krakiwski, 1986). The free-air relation mostly occurs locally (Torge,
248 1989).

249 In the Bologna area, data acquired with the Interferometric Synthetic Aperture Radar
250 (InSAR) technique are available. In a previous work (Zerbini et al., 2007), a first
251 comparison was made between the GPS and InSAR subsidence rates which showed the
252 consistency of the two estimates. A recent analysis of InSAR observations (Ferretti,
253 T.R.E., 2009), allows a further comparison supporting the reduction in the subsidence
254 rate observed by GPS at the BOLG station. T.R.E. kindly provided us with the results of
255 their Permanent Scatterers (Ferretti et al., 2001) analysis for two different periods and
256 satellites images. Figure 4 (a) shows the InSAR results obtained using the ERS satellite

257 images for the period 1992-2000 and (b) the RADARSAT passes in the time frame 2003-
258 2007. The comparison between the two images indicates a major reduction in the
259 subsidence rate over the Bologna area in the latter period.

260 The stations around the Venice area (Fig. 3 f, g, h, i and j) show reasonable agreement
261 between the GPS and AG linear trends. However, it should be pointed out that the AG
262 series are still limited in time and the associated errors, in particular for Marghera and
263 Cavallino, located a few hundred meters from the sea shore, are rather large.

264 The main hydrological parameters used in this work are the integrated simplified
265 hydrological balances and the precipitation series as described in section 2.2. In order to
266 achieve an understanding of the long-period behavior of the regional hydrology, we
267 estimated the linear trend of the hydrological balance for all stations over the period
268 1998-2007. It was found that, over this decade, only the northern stations at Treviso
269 ($+362\pm 4$ mm/yr), Voltabarozzo ($+35\pm 3$ mm/yr) and Cavallino ($+38\pm 3$ mm/yr) gain water,
270 while in all other sites, the amount of water is decreasing. In particular, the stations
271 located in the Plain, south of the Po River (Medicina, Marina di Ravenna, Bologna and
272 Boretto), are characterized by large negative trends up to -500 mm/yr. The analysis of the
273 precipitation series shows similar results.

274

275 **5.0 Long-period oscillations**

276

277 Many authors have shown that short-period (seasonal) height and gravity oscillations
278 are related to seasonal mass variations (see, for example, Blewitt et al., 2001; van Dam et

279 al., 2001; Zerbini et al., 2007). On the other hand, long-period (multi year) variations are
280 not as yet well understood because of the limited length of most of the time series.

281 In order to identify long-period oscillations, both the GPS heights and the
282 hydrological series were detrended to derive the residuals (Fig. 5). Possible correlations
283 between these residuals were investigated. For the sake of clarity, we point out that we
284 identify as hydrological balance and precipitation residuals the detrended series of the
285 time integral values of the observed hydrological balance and precipitation respectively.
286 Linear regressions were calculated between the height and the corresponding
287 hydrological balance and precipitation residual values.

288 By considering the Marina di Ravenna and Medicina residuals (Fig. 5b and d), over
289 the long period (multiyear), we observe anticorrelation between the height and each of
290 the two hydrological parameters. Anticorrelation can be interpreted as the loading effect
291 on the Earth's crust caused by the hydrology. In particular, for the MSEL station, a
292 regression between the hydrological balance and the height residuals over the period
293 1996-2008 provides a ratio of -24.7 ± 0.7 (significant at 99% confidence level), which
294 implies that for an increase of 24.7 mm of hydrological balance there is 1 mm decrease in
295 height (loading effect). A similar result is obtained by using the precipitation data
296 (-18.6 ± 0.4 , 99% confidence level). At Marina di Ravenna, on the Adriatic coast, the
297 ratios turn out to be -7.9 ± 0.4 and -8.1 ± 0.2 for the hydrological balance and the
298 precipitation residuals respectively. Since this site is on the coast, the magnitude of the
299 loading effect turns out to be smaller than that of the inland site (van Dam et al., 1994), in
300 this case about a factor of 2-to-3 of that observed inland at Medicina. The BOLG station
301 height residuals are characterized by a positive although weak correlation, $+3.3 \pm 0.4$ and

302 +4.1±0.2, with the hydrological balance and precipitation residuals respectively. All the
303 northern stations exhibit positive correlation. Since correlation is not explained by
304 loading, different physical mechanisms shall be invoked. A possible explanation could be
305 provided by the buoyancy effect according to which an increase/decrease of the
306 groundwater amount in the soil would produce an increase/decrease of height. Also clay
307 swelling/shrinking on water uptake/loss may occur. The different observed behaviors can
308 be related to the different geological settings and to the environmental conditions.

309

310 **6.0 Regional analysis**

311

312 The residual series of the GPS heights and gravity were analyzed both individually
313 and in conjunction with hydrological parameters by means of the EOF and SVD
314 approaches. We performed an EOF analysis on the individual variables, namely GPS
315 height, precipitation and hydrological balance, in order to identify spatial and temporal
316 variability features at local and regional scales. Additionally, at Medicina, the EOF
317 analysis has been carried out between pairs of variables: GPS height and water table,
318 gravity and hydrology, GPS height and gravity. The SVD analysis has been applied to
319 detect common signals between GPS heights and precipitation as well as between GPS
320 heights and hydrological balance. The length of the time series is an important factor
321 because only three GPS stations are present for a decade or longer, while all the stations
322 are simultaneously available only from 2004.

323 In order to reduce the high-frequency variability, the analysis is performed on weekly
324 time series. The weekly values were obtained by averaging the original daily data. A

325 weekly mean was computed when at least four daily values were available. Gaps shorter
326 than three days were preliminarily interpolated using the Objective Analysis technique
327 (Gandin, 1965; Bretherton et al., 1976).

328 The EOF and SVD analyses require that all series be defined at the same epochs; the
329 time series were detrended over the common period. Since variables measured in
330 different units may be involved, all the residual time series were standardized to zero
331 mean and unit standard deviation.

332 In the following, several cases were considered. Since we are interested in
333 understanding the long-period variability observed both in the height and gravity data,
334 only the stations with observation periods longer than six years were analyzed. We point
335 out that the gaps in the EOFs series are mostly due to missing GPS data at the Boretto
336 station. We will discuss spatial patterns, i.e. the coefficients shown in Tables 2 through 5
337 for the EOF analysis and Tables 6 and 7 for the SVD method, and time components, i.e.
338 the curves shown in Figures 6 and 7 for the EOF and Figure 8 for the SVD. For each
339 case, we will comment only the two largest EOFs (EOF1 and EOF2) and SVDs (SVD1
340 and SVD2) because, in general, they explain most of the observed variance. However,
341 Tables 2 to 7 list the whole set of EOF and SVD spatial patterns.

342

343 **6.1 GPS height series**

344

345 *Case A - Five GPS stations (1999-2007)*

346

347 In this case, identified as case A, we analyse the GPS height time series of five
348 stations: MSEL, MEDI, Marina di Ravenna, BOLG and Boretto. These sites are located
349 in the southern part of the region and are characterized by the longest data records,
350 spanning about eight years, from 1999 to the end of 2007. Concerning EOF1, the spatial
351 pattern shows that all stations behave coherently (Table 2). A height increase is observed
352 starting 2004-2005. A clear seasonality is superimposed with summer maxima and winter
353 minima (Fig. 6a). The spatial pattern of EOF2 is characterized by opposite behaviours of
354 Medicina (both MSEL and MEDI) and Boretto on one side, and Marina di Ravenna and
355 BOLG on the other. The EOF2 time component also shows a long-term signal, the slope
356 inversion starting around 2004.

357

358 *Case B - Eight GPS stations (2001-2007)*

359

360 Here we consider the stations of the previous case plus Cavallino, San Felice and
361 Voltabarozzo. In this case, called case B, eight stations are simultaneously available for a
362 period of about six years, from 2001 through the end of 2007, thus allowing us to extend
363 the analysis to the northern part of the region. Both EOF1 and EOF2 time components
364 show a long-term change starting around 2004-2005 (Fig. 6b). However, the EOF1
365 spatial pattern exhibits a different behaviour if we compare the northern and southern
366 stations (Table 3): while the northern sites have winter height maxima, the southern ones,
367 except BOLG, exhibit minima. Instead, the EOF2 spatial pattern is coherent across the
368 whole region.

369

370 **6.2 Precipitation time series**

371

372 The two cases described previously for the GPS heights are now considered for the
373 precipitation time series. It shall be pointed out that, for the Medicina site, we deal with a
374 unique precipitation series since the two GPS receivers (MEDI and MSEL) are separated
375 by 30 m only. Moreover, for Marghera, the precipitation data are not available.
376 Therefore, we will analyze two cases with four and seven stations respectively. Both
377 analyses show that EOF1 explains at least 75% of variance.

378

379 *Four precipitation stations (1999-2007)*

380

381 The Medicina, Marina di Ravenna, Bologna and Boretto precipitation series are
382 analyzed during the period 1999-2007. These precipitation stations are identified in the
383 relevant Tables with the abbreviations ME, RA, BO and BR respectively. EOF1 is
384 characterized by a coherent spatial pattern and by significant interannual fluctuations
385 (Table 4 and Fig. 7a). Considerable precipitation minima are found in 1999, 2002, 2003
386 and 2007 and maxima during the winters 1999-2000, 2002-2003 and during most of
387 2006. In Medicina and Bologna, EOF2 exhibits a decrease until 2003-2004, followed by
388 an increase; the opposite is found in Marina di Ravenna and Boretto.

389

390 *Seven precipitation stations (2001-2007)*

391

392 Cavallino, San Felice and Voltabarozzo precipitation time series are considered in
393 addition to the four stations mentioned above; in the Tables they are identified by means
394 of the following abbreviations: CA, SF and VO respectively. The results are quite similar
395 to those of the previous case (Table 5 and Fig. 7b).

396

397 **6.3 Hydrological Balance time series**

398

399 We analyzed also the hydrological balance time series by following the same scheme
400 used for the precipitation data described above. EOF1s, explaining about 90% variance,
401 are characterized by spatial coherence over the entire region. The related time
402 components exhibit a clear seasonality. The EOF2s are comparatively much smaller than
403 those in the case of precipitation.

404

405 **6.4 GPS height and precipitation**

406

407 The coupled variability of GPS height and hydrological variables (precipitation and
408 hydrological balance) is studied by using the SVD approach. Within the SVD analysis we
409 also distinguish two cases.

410

411 *Five GPS and four precipitation stations (1999-2007)*

412

413 We analyze the GPS heights of case A together with the Medicina, Marina di
414 Ravenna, Bologna and Boretto precipitation series for the period 1999-2007. SVD1

415 explains 81% covariance; the precipitation spatial pattern is characterized by coherence
416 (Table 6b). The GPS height spatial pattern is anticorrelated with precipitation at Medicina
417 (both MSEL and MEDI) and Boretto, while RA and BOLG do not show significant
418 correlation (Table 6a). Both time components exhibit a long-period fluctuation, with a
419 minimum around 2003-2004 (Fig. 8a), superimposed to which are seasonal oscillations.
420 The anticorrelation can be interpreted as a loading/unloading effect on the Earth's crust
421 caused by variations in the precipitation regime. The SVD2 spatial pattern of the GPS
422 height mostly exhibits regional coherence. Both time components show a long-term
423 fluctuation with a seasonal signal superimposed. GPS is characterized by decreasing
424 heights until beginning of 2004 and by an increase afterwards.

425 The correlation coefficients between the relevant SVD time components turn out to
426 be 0.45 for SVD1 and 0.65 for SVD2, SVD1 significant at 93% confidence level while
427 SVD2 significance is greater than 99%.

428

429 *Eight GPS and seven precipitation stations (2001-2007)*

430

431 Here we analyze the GPS heights of case B together with the seven precipitation
432 series mentioned above. The time span thus reduces to 2001-2007. The covariance
433 explained by SVD1 amounts to about 92%. The precipitation spatial pattern is coherent
434 (Table 7b), while the GPS height pattern is characterized by a dipole (Table 7a). As
435 regards the northern stations, GPS heights are correlated with precipitation, while the
436 southern ones are anti-correlated. SVD2 shows a low percentage of covariance (6%). A
437 long-term fluctuation is clearly recognizable in both SVDs with characteristics similar to

438 those of the previous case (Fig. 8b). Here, the correlation coefficients are 0.45 for SVD1
439 and 0.64 for SVD2, the first is significant at 90% confidence level while the significance
440 of the second is 98%.

441 Since SVD1 explains more than 90% of the signal and the GPS height pattern
442 exhibits a well-defined south-north asymmetry, we further investigated the relationship
443 between the GPS height and precipitation. After estimating the average standard
444 deviations of the two parameters for the southern and northern parts of the region
445 respectively, we have computed the relevant ratios indicative of the height response to
446 precipitation variations. In the south, the ratio turns out to be 1 mm of height for 20 mm
447 of precipitation. In the north the ratio is instead 1/35. Because, by definition, the standard
448 deviation is a positive quantity, the signs are deduced from those of the relevant SVD1
449 spatial patterns (Table 7); therefore in the south the sign of the ratio is negative whereas
450 in the north it is positive. These values are in agreement with those derived by means of
451 linear regressions between height and precipitations residuals (see section 5.0). If we
452 assume a 1 mm homogeneous increase of precipitation over the entire area, there would
453 be about 0.05 mm height decrease in the southern part while a height increase of about
454 0.03 mm would occur in the north.

455

456 **6.5 GPS height and hydrological balance**

457

458 The coupled variance between GPS height and hydrological balance exhibits results
459 quite similar to those obtained by using precipitation. In all these analyses, the SVD1s
460 explain a slightly larger covariance compared to the same cases involving precipitation.

461 The spatial patterns of the hydrological balance are always regionally coherent; however,
462 as in section 6.4, the GPS heights of the northern stations are correlated with the
463 hydrological balance, while the southern ones are anti-correlated except for BOLG.

464

465 **7.0 Local scale analysis - Medicina**

466

467 At Medicina, time series of various parameters are acquired continuously for more
468 than a decade now, GPS height (MSEL and MEDI stations), SG gravity, water table data
469 and other environmental information. This makes it possible to compare locally the
470 different series. A few examples are provided, namely we correlate, by means of the EOF
471 analysis, GPS height (both MEDI and MSEL) with water table, SG gravity with
472 precipitation and water table respectively and GPS height and SG gravity. Tables 8
473 through 10 present the pattern coefficients while the time components are presented in
474 Figures 9, 10 and 11.

475

476 **7.1 GPS height and water table**

477

478 The two GPS height data sets, MSEL and MEDI, exhibit the same response to the
479 water table variations (Fig. 9a and b, Table 8a and b). Both EOF1s are clearly
480 representative of the loading/unloading effect caused by the seasonal water table
481 variations. We observe maxima in the summer when the water table decreases and
482 minima in the winter when the water table rises close to the topographic surface. This
483 comparison also allows identifying a height decrease starting in 2002-2003 followed by a

484 height increase starting at the end of 2005. These long-period height variations are
485 correlated with increase/decrease in the water table level as a consequence of changes in
486 the precipitation regime.

487

488 **7.2 SG gravity and hydrology**

489

490 We have compared the SG data series with those of precipitation and water table. The
491 results provided by the two cases are similar (Fig. 10a and b; Table 9a and b), although
492 the SG data are slightly more correlated with the water table variations (63.6% PVE) than
493 to those of precipitation (52.7% PVE). Both EOF1s show a clear seasonal signal with
494 summer minima and winter maxima likely resulting from the combination of two effects:
495 the variations in gravity due to the Newtonian mass attraction and to height fluctuations.
496 In fact, the EOF1s pattern coefficients have the same sign indicating on the one hand that
497 to an increase/decrease of water mass corresponds an increase/decrease of gravity; on the
498 other hand an increase of water/precipitation will load the crust inducing a height
499 decrease, which turns into a gravity increase. In the case of the EOF2s, we can notice a
500 long-period signal starting at the beginning of 2002-2003. The pattern coefficients of
501 EOF2s have opposite sign; this mode could be explained by invoking a variation in
502 gravity due to a height change resulting from a buoyancy effect and/or a soil
503 consolidation process. In this latter case, a decrease of the water content in the soil will
504 cause a height decrease which, in turn, will result into a gravity increase. The soil
505 consolidation phenomenon is known to occur particularly in clayey soils such as that
506 present at Medicina (Romagnoli et al., 2003).

507

508 **7.3 GPS height and SG gravity**

509

510 The EOF1s time components for MEDI and MSEL show a clear seasonal signal both
511 in GPS heights and SG time series (Fig. 11a and b) as well as a long-period feature
512 starting at the beginning of 2005. The pattern coefficients are of opposite sign (Table 10a
513 and b), thus indicating anticorrelation between the two variables for the EOF1s. This
514 means that the seasonal maxima and minima of GPS heights and SG gravity are opposite
515 in phase as expected, and that, on a longer period of time, to the height increase starting
516 in 2005 corresponds a gravity decrease. The EOF2s indicate the presence of a long-period
517 oscillation with a minimum around 2002-2003. The pattern coefficients have the same
518 sign (Table 10a and b) suggesting that this mode could result from buoyancy and/or soil
519 consolidation effects.

520

521 **8.0 Comparisons**

522

523 We compared, as an example, the original detrended GPS height series and the
524 reconstructed signals by means of the main EOFs components for the two cases A and B
525 (see section 6.1). According to our arbitrary choice, the reconstructed signals must
526 explain at least 70% of the observed variance. Therefore, three EOFs were used in case
527 A, thus accounting for 70.2% of the variance (Table 2 and Fig. 12). In case B, five EOFs
528 were selected which represent 78.9% of the variance (Table 3 and Fig. 13). For the
529 stations which are common to cases A and B, there are no major differences between the

530 two EOF reconstructions. However, it shall be noticed that in case A (Fig. 12) Marina di
531 Ravenna shows, in the period 2004-2006 a minor discrepancy between the observed
532 height residuals and the reconstructed signal, which does not appear in case B (Fig. 13).
533 This difference might be due to the fact that the reconstruction of the signal in case B is
534 accomplished through a slightly larger variance (78.9%) with respect to A (70.2 %). In
535 case B, the analysis is also covering a larger area with respect to A; this might imply the
536 presence of an additional regional component.

537

538 **9.0 Conclusions**

539

540 Over northeastern Italy, starting around 2004-2005, a reduction of the subsidence
541 rates has been observed in conjunction with a decrease of the hydrological load on the
542 Earth's crust mostly due to a decrease in the amount of precipitation.

543 The EOF and SVD analyses of the residuals of the GPS heights, hydrological
544 parameters and gravity made it possible to identify long and short period oscillations and
545 also to recognize common features in different pairs of variables. These findings,
546 obtained by means of purely mathematical approaches, are supported by sound physical
547 interpretation that allows to point at the local/regional hydrology as one of the main
548 contributors to the observed height oscillations. Since a percentage of variance or
549 covariance is associated to each EOF or SVD component respectively, the mathematical
550 decomposition of the time series, together with the physical interpretation, provides a
551 means to attribute a relative weight to the different phenomena involved.

552 In both the analyzed A and B cases (section 6.1), the time components of the main
553 EOFs show a slope inversion starting around 2004-2005. In particular, a coherent height
554 increase is found by EOF1 in case A (Fig. 6a, Table 2) and by EOF2 in case B (Fig. 6b,
555 Table 3). Also the EOF1 spatial pattern in case B clearly indicates an opposite north-
556 south behavior of the station heights on the short as well as on the multi-year period
557 (Table 3). For example, at seasonal scale, this means that summer height maxima of the
558 stations in the southern Po Plain are mirrored by height minima in the northern part of the
559 region. Case B, which involves a larger spatial domain with respect to case A, has made
560 it possible to recognize a regional signal.

561 As regards precipitation, the EOF1s of both the four and seven station cases
562 (section 6.2) show a marked decrease in the precipitation residuals starting at the end of
563 2005 (Fig. 7a and b and Tables 4 and 5).

564 The SVD analysis of the GPS heights and precipitation series has demonstrated
565 the high spatial covariance and the high time correlation between these two parameters.
566 The SVD1 in both analyses indicates that the GPS heights of the sites in the southern Po
567 Plain are anticorrelated with precipitation, while the northern sites are positively
568 correlated. We have interpreted anticorrelation as the loading/unloading effect on the
569 Earth's crust exerted by the increase/decrease in precipitation, which occurs in the period
570 2002-2005 and 2006-2008 respectively (Fig. 8). The reduction in the precipitation regime
571 observed, for example, from the end of 2005, unloads the crust and it turns into a height
572 increase particularly at the stations located in the southern Po Plain which are
573 characterized mostly by clayey soils.

574 The opposite response to hydrological loading of the southern and northern parts
575 of the region under investigation (see 6.1, case B and 6.4 “eight GPS and seven
576 precipitation stations”) results in a south-north height gradient, which turns out to be in
577 the order of 0.1 mm over a distance of about 100 km, by assuming a 1 mm homogeneous
578 increase of precipitation over the entire area. When observing and studying crustal
579 deformation of a region, it is important to identify how the height of the stations changes
580 in response to the hydrological load, in particular when weak tectonic signals are being
581 sought.

582 At Medicina, a few comparisons were made, namely between GPS heights and
583 water table, SG gravity data and hydrology and between GPS heights and SG gravity
584 (Fig. 10). In all three cases, the EOF1s time components are characterized by a clear
585 seasonal signal. This is due to loading/unloading of the crust in the case of the GPS
586 height variations and to variations of Newtonian mass attraction and height in the case of
587 gravity. GPS height and SG gravity show a marked common seasonal signal as well as a
588 long-term fluctuation (Fig. 11) pointing to a height increase which is quite evident
589 starting from the end of 2005.

590

591 **References**

592

593 Altamimi, Z., X. Collilieux, J. Legrand, B. Garayt and C. Boucher (2007), ITRF2005: A
594 new release of the International Terrestrial Reference Frame based on time series of
595 station positions and Earth Orientation Parameters, *J. Geophys. Res.*, 112, B09401,
596 doi:10.1029/2007JB004949.

597

598 Björnsson, H. and S. Venegas (1997), A Manual for EOF and SVD Analyses of Climate
599 Data. CCGCR Report No. 97-1, Montréal, 52 pp (available from www.awi.de).

600

601 Blewitt, G., D. Lavallée, P. Clarke and K. Nurutdinov (2001), A new global mode of
602 Earth deformation: Seasonal cycle detected, *Science*, 294, 2342– 2345.

603

604 Bretherton, F. P., R. E. Davis, and C. B. Fandry (1976), A technique for objective
605 analysis and design of oceanographic experiments applied to MODE-73, *Deep-Sea Res.*,
606 23, 559–582.

607

608 Bretherton, C.S., C. Smith, and J.M. Wallace (1992), An intercomparison of methods for
609 finding coupled patterns in climate data. *J. Climate*, 5, 541–560.

610

611 Carminati, E. and G. Di Donato, (1999), Separating natural and anthropogenic vertical
612 movements in fast subsiding areas: the Po Plain (N. Italy) case. *Geophys. Res. Lett.* 26,
613 2291–2294.

614

615 Carminati, E. and G. Martinelli (2002), Subsidence rates in the Po Plain, northern Italy:
616 the relative impact of natural and anthropogenic causation. *Engineering Geology*, 66, 241–
617 255.

618

- 619 Carminati, E., C. Doglioni, and D. Scrocca (2003), Apennines subduction related
620 subsidence of Venice (Italy), *Geophys. Res. Lett.*, 30(13), 1717,
621 doi:10.1029/2003GL017001.
- 622
- 623 Dach, R., U. Hugentobler, P. Fridez and M. Meindl (2007), Bernese GPS Software
624 version 5.0, Stämpfli Publications AG Bern, 612 pp.
- 625
- 626 Ferretti, A., C. Prati and F. Rocca (2001), Permanent Scatterers in SAR interferometry,
627 *IEEE Trans Geosci. Remote Sens.*, 39, 8-20.
- 628
- 629 Ferretti, A., T.R.E. (Tele-Rilevamento Europa T.R.E. srl) (2009), Private communication.
- 630
- 631 Gandin, L. S. (1965), Objective Analysis of Meteorological Fields, Israel Program for
632 Scientific Translations, 242 pp.
- 633
- 634 Hannachi, A. (2004), A Primer for the EOF Analysis of Climate Data, Department of
635 Meteorology, University of Reading, UK, 33pp (Available from: ncas-cms.nerc.ac.uk)
- 636
- 637 Hargreaves, G.H. and Z.A. Samani (1982), Estimating potential evapo-transpiration. *J.*
638 *Irrig and Drain Engr.*, ASCE, 108 (IR3), 223-230.
- 639
- 640 Hargreaves, G.H. and Z.A. Samani (1985), Reference crop evapo-transpiration from
641 temperature. *Transactions of ASAE*, 1 (2), 96-99.

642

643 Pignone, R., U. Cibin, P. Severi (2008), Pianura bolognese e costa le aree più critiche,
644 Supplemento al N. 1, anno XI, ARPA Rivista, gennaio-febbraio 2008, Il monitoraggio
645 della subsidenza - Esperienze a confronto, 8-9.

646

647 Romagnoli, C., S. Zerbini, L. Lago, B. Richter, D. Simon, F. Domenichini, C. Elmi, M.
648 Ghirotti (2003), Influence of soil consolidation and thermal expansion effects on height
649 and gravity variations, Journ. of Geodynamics, 35, N. 4-5, 521-539.

650

651 Szafranek, K. and A. Kenyeres (2009), Private communication.

652

653 Torge, W., (1989), Gravimetry, W. De Gruyter, 465 pp.

654

655 Van Dam, T.M., G. Blewitt, M.B. Heflin (1994), Atmospheric pressure loading effects on
656 Global Positioning System coordinate determinations, J. Geophys. Res., 99(B12), 23.939-
657 23.950.

658

659 van Dam, T. M., J. Wahr, P.C.D. Milly, A. B., Shmakin, G. Blewitt, D. Lavallée and K.
660 M. Larson (2001), Crustal displacements due to continental water loading, Geophys. Res.
661 Lett., 28, 4, 651-654, doi: 10.1029/2000GL012120.

662

663 Vaníček, P. and E.J. Krakiwski (1986), Geodesy: the concepts, North-Holland,
664 Amsterdam, 697 pp.

665

666 Venegas, S.A. (2001) Statistical Methods for Signal Detection in Climate. DCESS Report
667 No. 2, Niels Bohr Institute for Astronomy, Physics and Geophysics, University of
668 Copenhagen, 96 pp.

669

670 von Storch, H., and A. Navarra (Eds.) (1999), Analysis of Climate Variability:
671 Applications of Statistical Techniques, Springer Verlag, Berlin, 342 pp.

672

673 Zerbini, S., B. Richter, M. Negusini, D. Simon, C. Romagnoli and F. Domenichini
674 (2000), Vertical crustal motions and mean sea level: an experiment in the Eastern Po
675 Plain, in Land Subsidence, Proceedings of the Sixth International Symposium on Land
676 Subsidence, 24-29 September 2000, Ravenna, Italy, L. Carbognin, G. Gambolati A.I.
677 Johnson eds., ISBN 88-87222-06-1, vol. II, 151-163.

678

679 Zerbini S., M. Negusini, C. Romagnoli, F. Domenichini, B. Richter, D. Simon (2002),
680 Multi-parameter continuous observations to detect ground deformation and to study
681 environmental variability impacts, Global and Planetary Change 34, 37–58.

682

683 Zerbini S., B. Richter, F. Rocca, T. van Dam, F. Matonti, (2007), Combination of space
684 and terrestrial geodetic techniques to monitor land subsidence: Case study, the
685 southeastern Po Plain, Italy, Journ. Geophys. Res. Solid Earth, 112, B05401,
686 doi:10.1029/2006JB004338.

687

688 **Acknowledgments**

689

690 This work has been developed in the frame of the IGCP 565 project “Developing the
691 Global Geodetic Observing System into a Monitoring System for the Global Water
692 Cycle”. The authors are grateful to Dr. Erika De Simone for having contributed to the
693 analysis of the GPS data and to Dr. Hartmut Wziontek and Eng. Peter Wolf for the
694 analysis of the SG gravity data. We would like to thank Prof. A. Ferretti and T.R.E. for
695 having provided the InSAR results. We also would like to thank Drs. K. Szafranek. and
696 A. Kenyeres for having provided the weekly EUREF GPS height solutions of the MEDI
697 station. The authors are also grateful to two unknown reviewers the comments and
698 suggestions of which helped us to improve the manuscript.

699

700 Figure Captions

701

702 Figure 1. Map of station locations in northeastern Italy. Bologna, Loiano, Marina di
703 Ravenna, Medicina (MSEL) are stations of the GPS network run by the University of
704 Bologna; Boretto belongs to Telespazio; Cavallino, Marghera, San Felice, Treviso and
705 Voltabarozzo are stations of the GPS network run by Consorzio Venezia Nuova for the
706 Magistrato alle Acque of Venice; the MEDI station belongs to the Italian Space Agency.

707

708 Figure 2. Medicina: daily water table (cyan line), hydrological balance (red line) and
709 precipitation (black line) data.

710

711 Figure 3. Time series of GPS heights and gravity; they are ordered from south to north.
712 Panel a) Loiano (LOIA) daily GPS height (purple line); b) Marina di Ravenna (RA)
713 daily GPS height (red line); c) Bologna (BOLG) daily GPS height (blue line) and a series
714 of AG measurements (red dots); d) Medicina GPS heights: MEDI (magenta line, EUREF
715 weekly solution) and MSEL (olive line, daily solution); daily SG time series (blue line)
716 and AG measurements (red dots); e) Boretto (BR) daily GPS height (dark yellow line); f)
717 San Felice (SF) daily GPS height (wine line); g) Voltabarozzo (VO) daily GPS height
718 (dark green line) and AG measurements (red dots); h) Marghera (MA) daily GPS height
719 (dark blue line) and AG measurements (red dots); i) Cavallino (CA) daily GPS height
720 (orange line) and AG measurements (red dots); j) Treviso (TV) daily GPS height (violet
721 line) and AG measurements (red dots). In all panels, gravity is multiplied by (-1).

722

723 Figure 4. InSAR maps of the terrain deformation in the Bologna area; (a) ERS
724 descending passes in the period 1992-2000 and (b) Radarsat descending passes during
725 2003-2007.

726

727 Figure 5. GPS height, precipitation (black line) and hydrological balance (cyan line)
728 residuals. GPS: Panel a): LOIA (purple line); b) RA (red line); c) BOLG (blue line); d)
729 MSEL (olive line) and MEDI (magenta line); e) BR (dark yellow line); f) SF (wine line);
730 g) VO (dark green line); h) MA (dark blue line); i) CA (orange line); j) TV (violet line).

731

732 Figure 6. EOF1 and EOF2 time components of GPS height residuals. Panel a) Five GPS
733 stations: MSEL, MEDI, RA, BOLG and BR; b) Eight GPS stations: MSEL, MEDI, RA,
734 BOLG, BR, CA, SF and VO.

735

736 Figure 7. EOF1 and EOF2 time components of precipitation residuals. Panel a) Four
737 precipitation stations: Medicina (ME), Marina di Ravenna (RA), Bologna (BO) and
738 Boretto (BR); b) Seven precipitation stations: ME, RA, BO, BR, Cavallino (CA), San
739 Felice (SF) and Voltabarozzo (VO).

740

741 Figure 8. SVD1 and SVD2 time components of the variable pair GPS height (blue dots)
742 and precipitation residuals (red dots). Panel a) Five GPS stations (MSEL, MEDI, RA,
743 BOLG and BR) and four precipitation stations (ME, RA, BO and BR); b) Eight GPS
744 stations (MSEL, MEDI, RA, BOLG, BR, CA, SF and VO) and seven precipitation
745 stations (ME, RA, BO, BR, CA, SF and VO).

746

747 Figure 9. EOF1 and EOF2 time components of the Medicina GPS height and water table
748 residuals. Panel a) MEDI and water table; b) MSEL and water table.

749

750 Figure 10. EOF1 and EOF2 time components of the Medicina superconducting
751 gravimeter (SG) and local hydrology residuals: Panel a) SG and precipitation; b) SG and
752 water table.

753

754 Figure 11. EOF1 and EOF2 time components of the Medicina GPS height and
755 superconducting gravimeter (SG) residuals. Panel a) MEDI and SG; b) MSEL and SG.

756

757 Figure 12. EOF reconstruction and observed height residuals. Five GPS stations: Panel a)
758 RA, observed height residuals (red line) and EOF reconstruction (green line); b) BOLG
759 (blue and purple); c) MSEL (olive and orange); d) MEDI (magenta and navy) and e) BR
760 (dark yellow and cyan). The reconstruction is based on the first three EOFs and explains
761 70.2% of the total variance.

762

763 Figure 13. EOF reconstruction and observed height residuals. Eight GPS stations: Panel
764 a) RA, observed height residuals (red line) and EOF reconstruction (green line); b)
765 BOLG (blue and purple); c) MSEL (olive and orange); d) MEDI (magenta and navy); e)
766 BR (dark yellow and cyan); f) SF (grey and pink); g) VO (wine and yellow) and h) CA
767 (dark cyan and black). The reconstruction is based on the first five EOFs and explains
768 78.9% of the total variance.

769

770

Table Captions

771

772 Table 1.

773 List of stations, North/South regional identifier, techniques available and linear trends of
774 the GPS height, Superconducting Gravimeter (SG) and Absolute Gravity (AG) series.

775 The formal error associated to the estimated trends, both for GPS heights and gravity,

776 have been multiplied by an arbitrary factor of 5 to provide conservative estimates of the

777 errors. The superscript (a) indicates that only one AG measurement is available at LOIA.

778 The superscript (b) indicates that the MEDI data are EUREF weekly solutions.

779

780 Table 2. EOF analysis of five GPS height residuals series (MSEL, MEDI, RA, BOLG
781 and BR). The second column lists the percentage of variance explained (PVE) by each

782 EOF, the following columns describe the spatial patterns.

783

784 Table 3. EOF analysis of eight GPS height residuals series (MSEL, MEDI, RA, BOLG,
785 BR, CA, SF and VO). The second column lists the percentage of variance explained

786 (PVE) by each EOF, the following columns describe the spatial patterns.

787

788 Table 4. EOF analysis of four precipitation residuals series (ME, RA, BO and BR). The
789 second column lists the percentage of variance explained (PVE) by each EOF, the

790 following columns describe the spatial patterns.

791

792 Table 5. EOF analysis of seven precipitation residuals series (ME, RA, BO, BR, CA, SF
793 and VO). The second column lists the percentage of variance explained (PVE) by each
794 EOF, the following columns describe the spatial patterns.

795

796 Table 6. SVD analysis of the variable pair GPS height (a) and precipitation residuals (b).
797 Five GPS stations (MSEL, MEDI, RA, BOLG and BR) and four precipitation stations
798 (ME, RA, BO and BR). The two stations at Medicina, MSEL and MEDI, are coupled to
799 the same ME precipitation data series. The second column lists the squared covariance
800 percentage relevant to each SVD, the following columns describe the spatial patterns.

801

802 Table 7. SVD analysis of the variable pair GPS height (a) and precipitation residuals (b).
803 Eight GPS stations (MSEL, MEDI, RA, BOLG, BR, CA, SF and VO) and seven
804 precipitation stations (ME, RA, BO, BR, CA, SF and VO). The two stations at Medicina,
805 MSEL and MEDI, are coupled to the same ME precipitation data series. The second
806 column lists the squared covariance percentage relevant to each SVD, the following
807 columns describe the spatial patterns.

808

809 Table 8. EOF analysis of two time series, GPS height and water table residuals, at
810 Medicina. The second column lists the percentage of variance explained (PVE) by each
811 EOF, the following columns describe the spatial patterns. (a) MSEL and water table; (b)
812 MEDI and water table.

813

814 Table 9. EOF analysis of two time series, superconducting gravimeter (SG) and local
815 hydrology residuals, at Medicina. The second column lists the percentage of variance
816 explained (PVE) by each EOF, the following columns describe the spatial patterns. (a)
817 SG and precipitation; (b) SG and water table.

818

819 Table 10. EOF analysis of two time series, GPS height and superconducting gravimeter
820 (SG) residuals, at Medicina. The second column lists the percentage of variance
821 explained (PVE) by each EOF, the following columns describe the spatial patterns. (a)
822 MEDI and SG; (b) MSEL and SG.

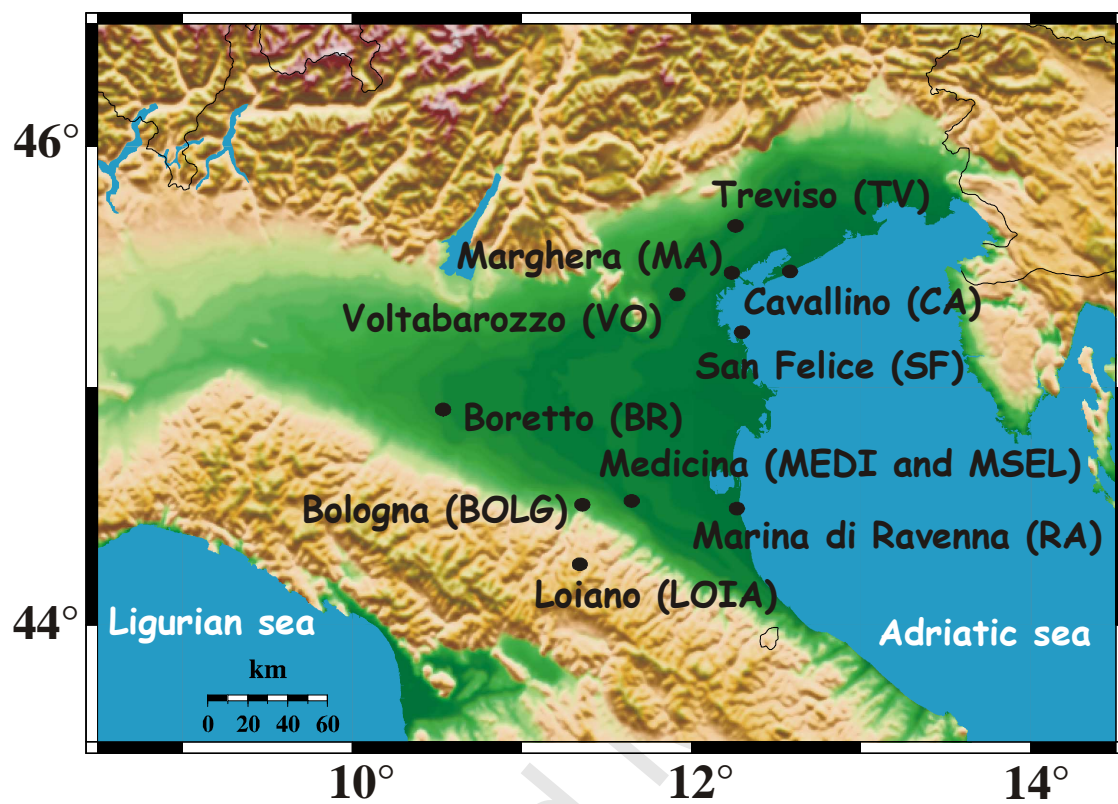


Figure 1

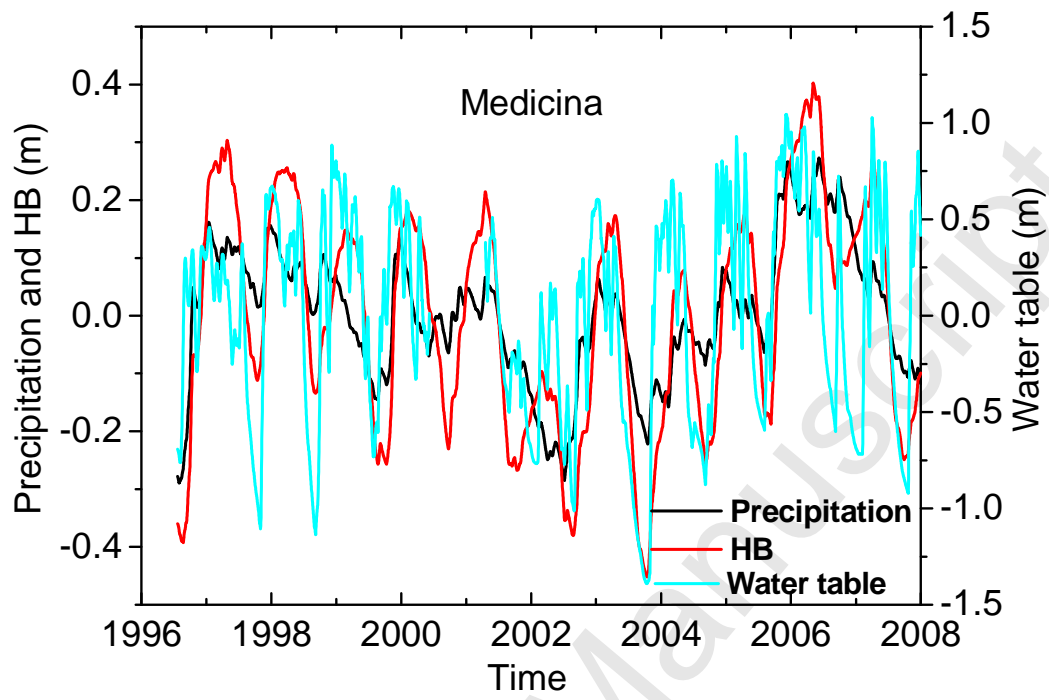


Figure 2

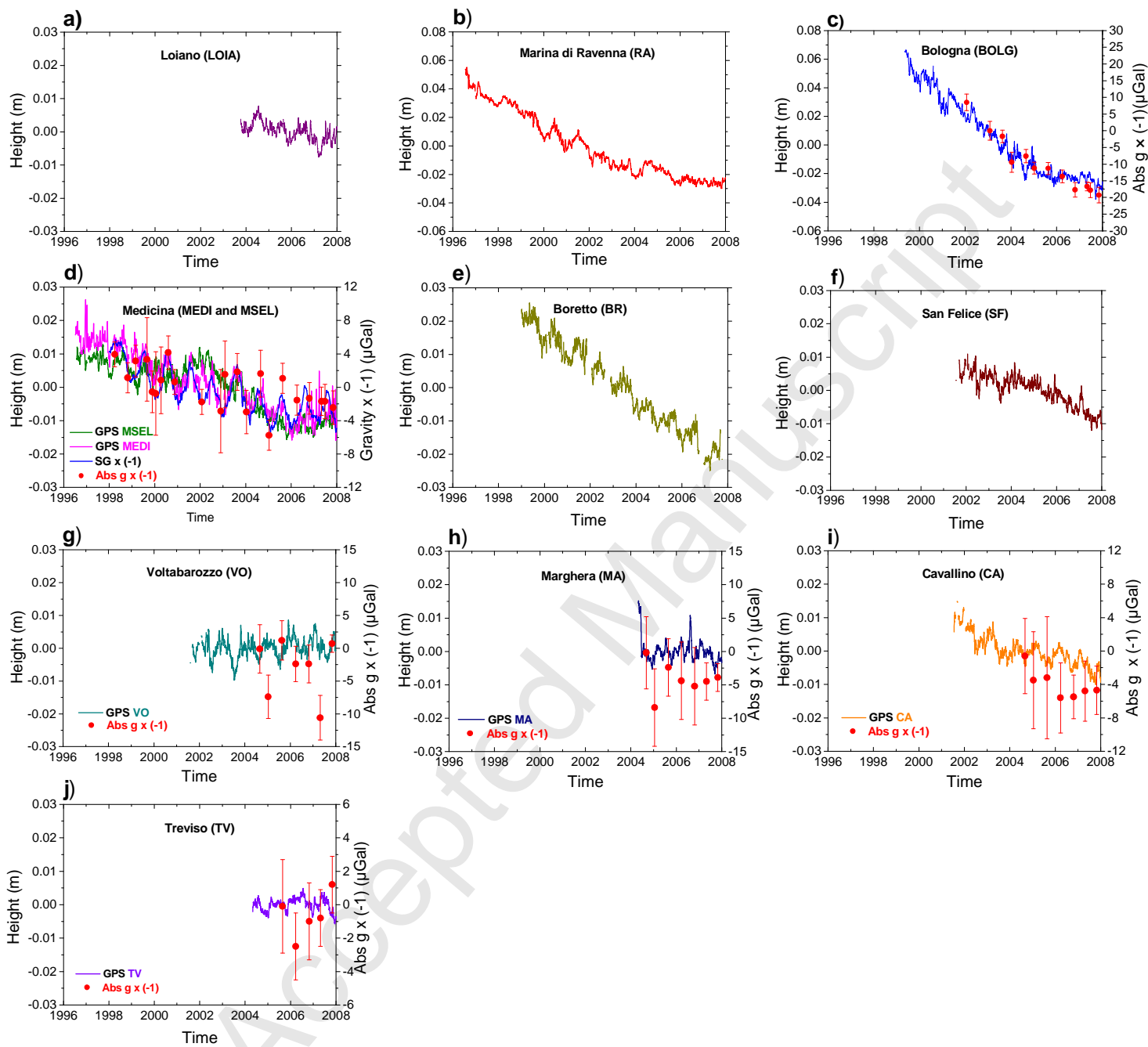


Figure 3

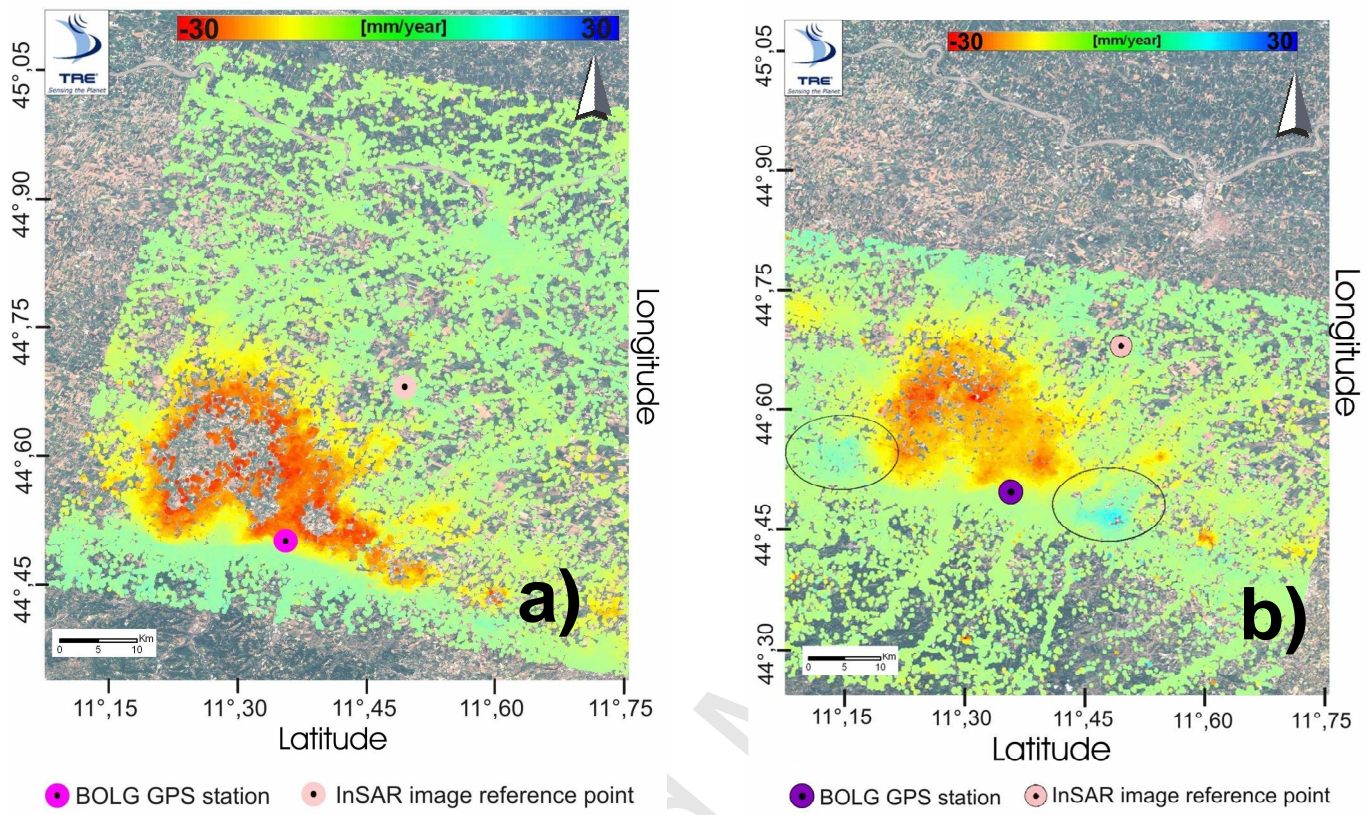


Figure 4

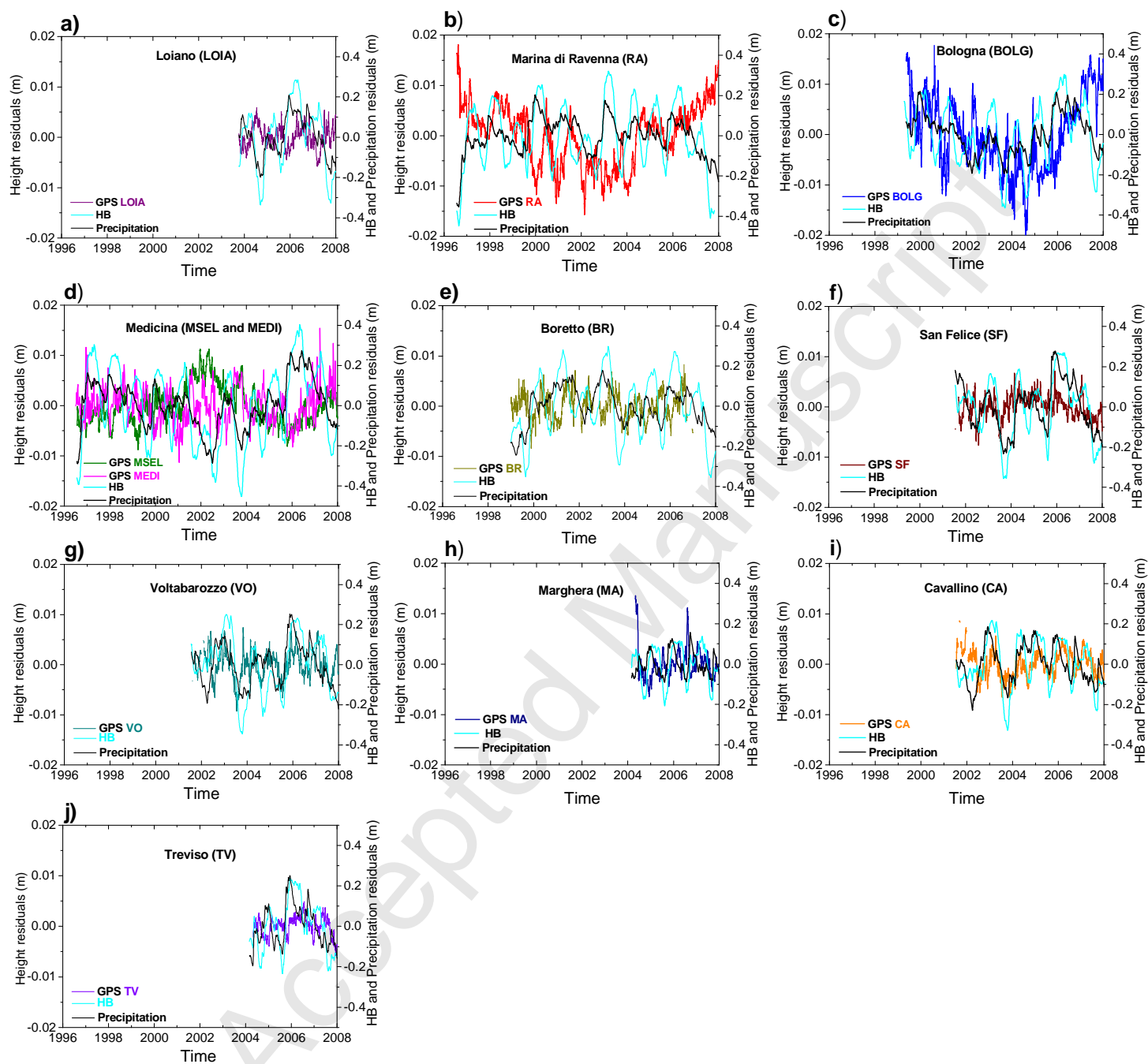


Figure 5

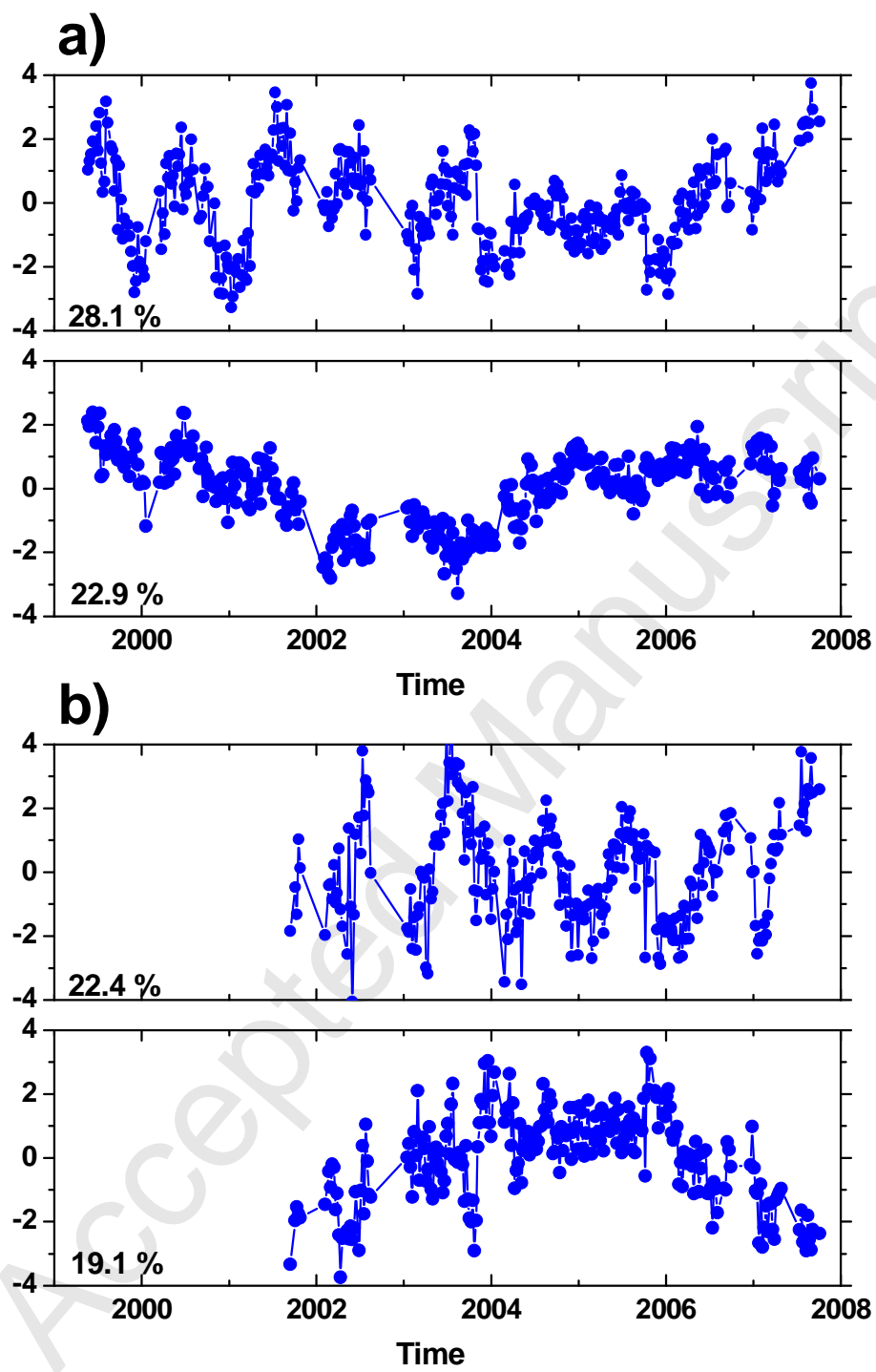


Figure 6

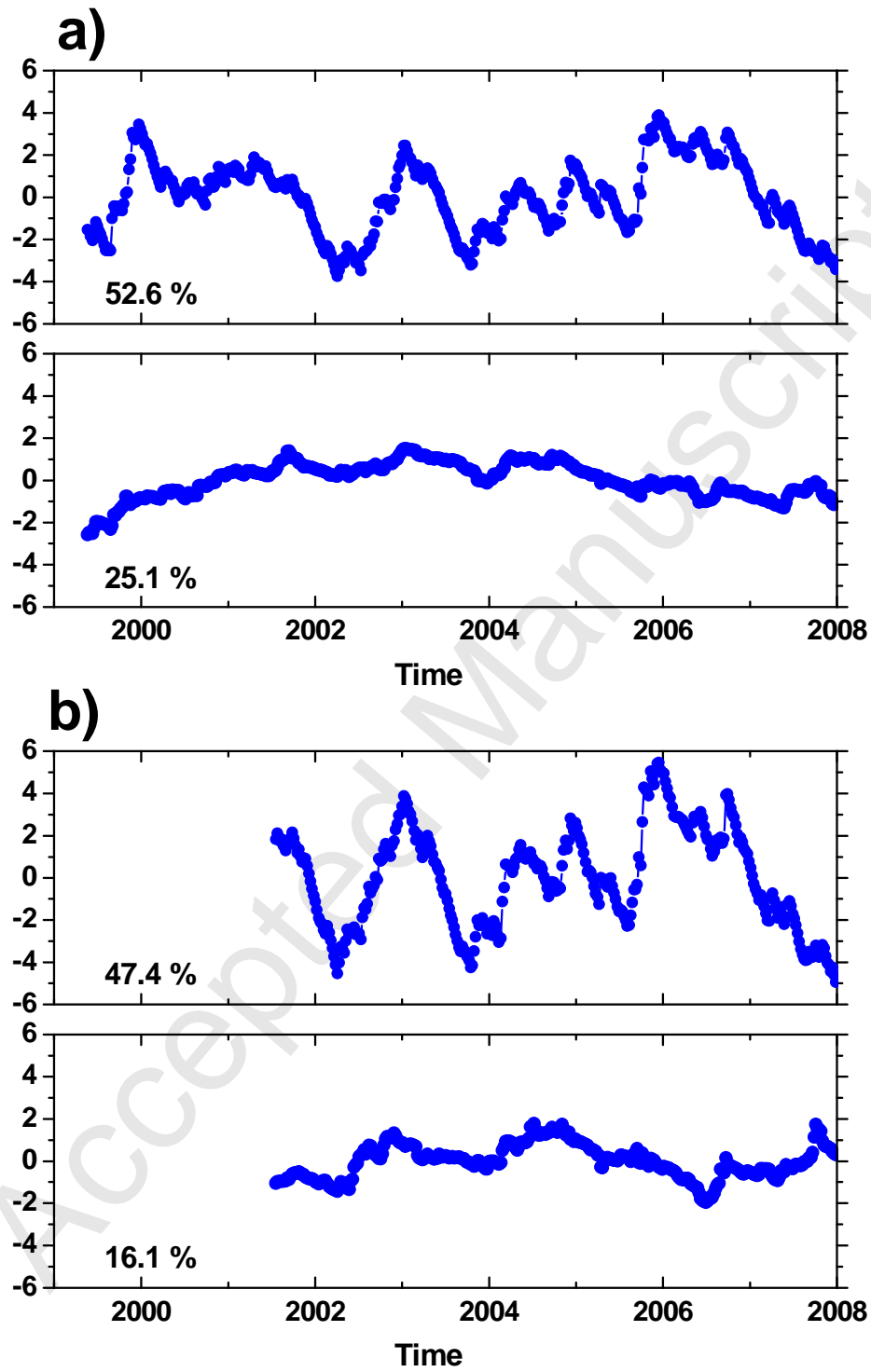


Figure 7

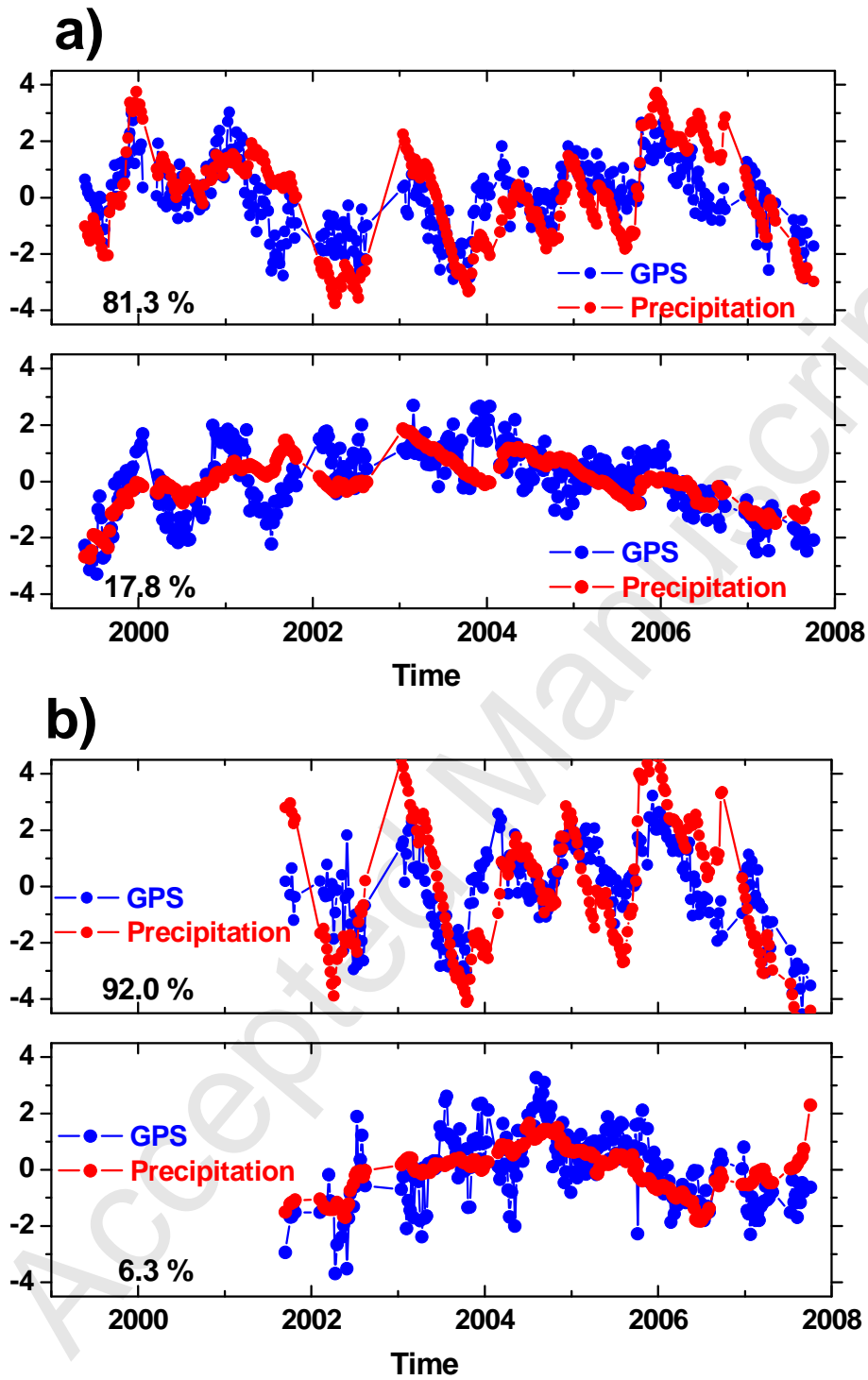


Figure 8

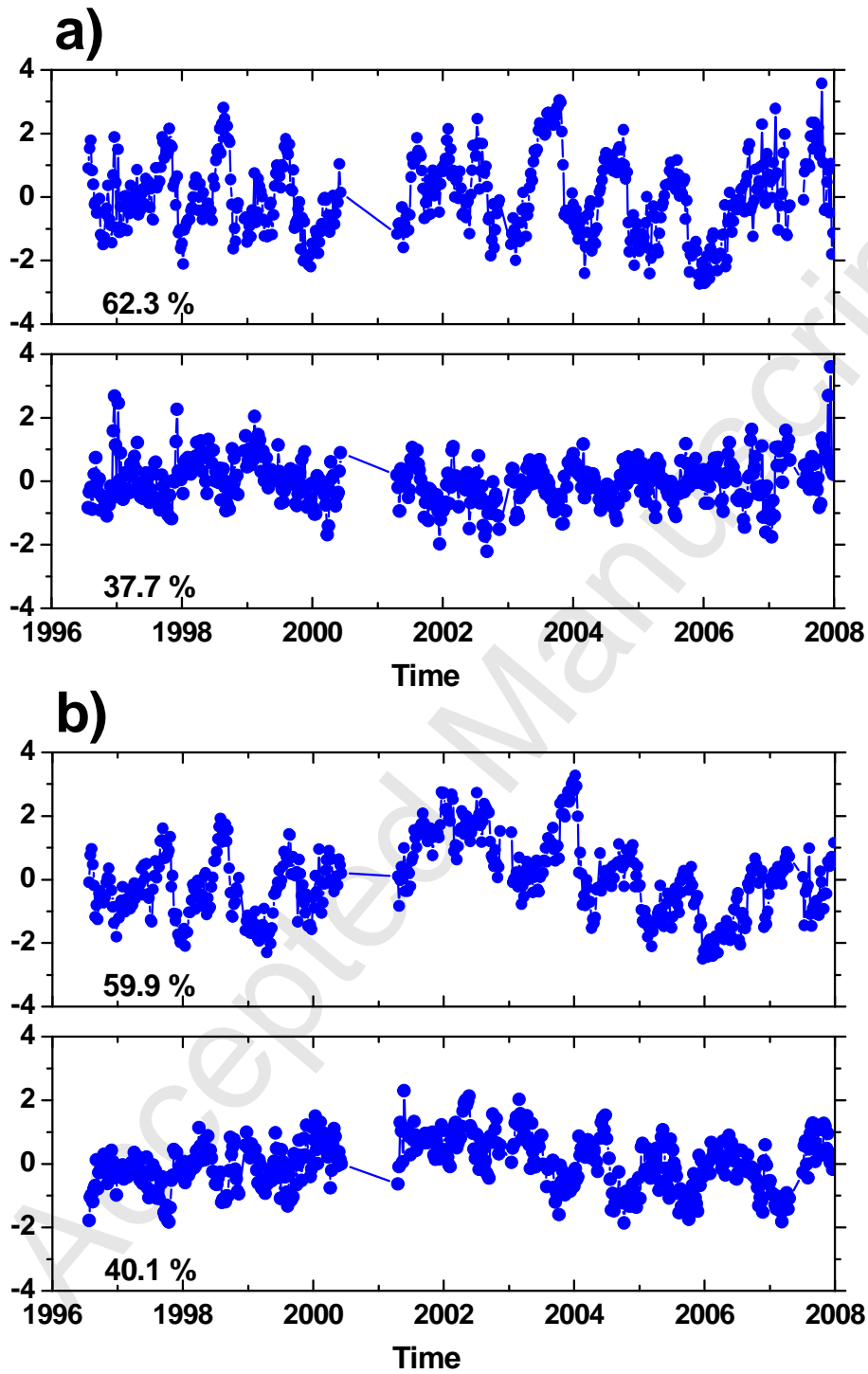


Figure 9

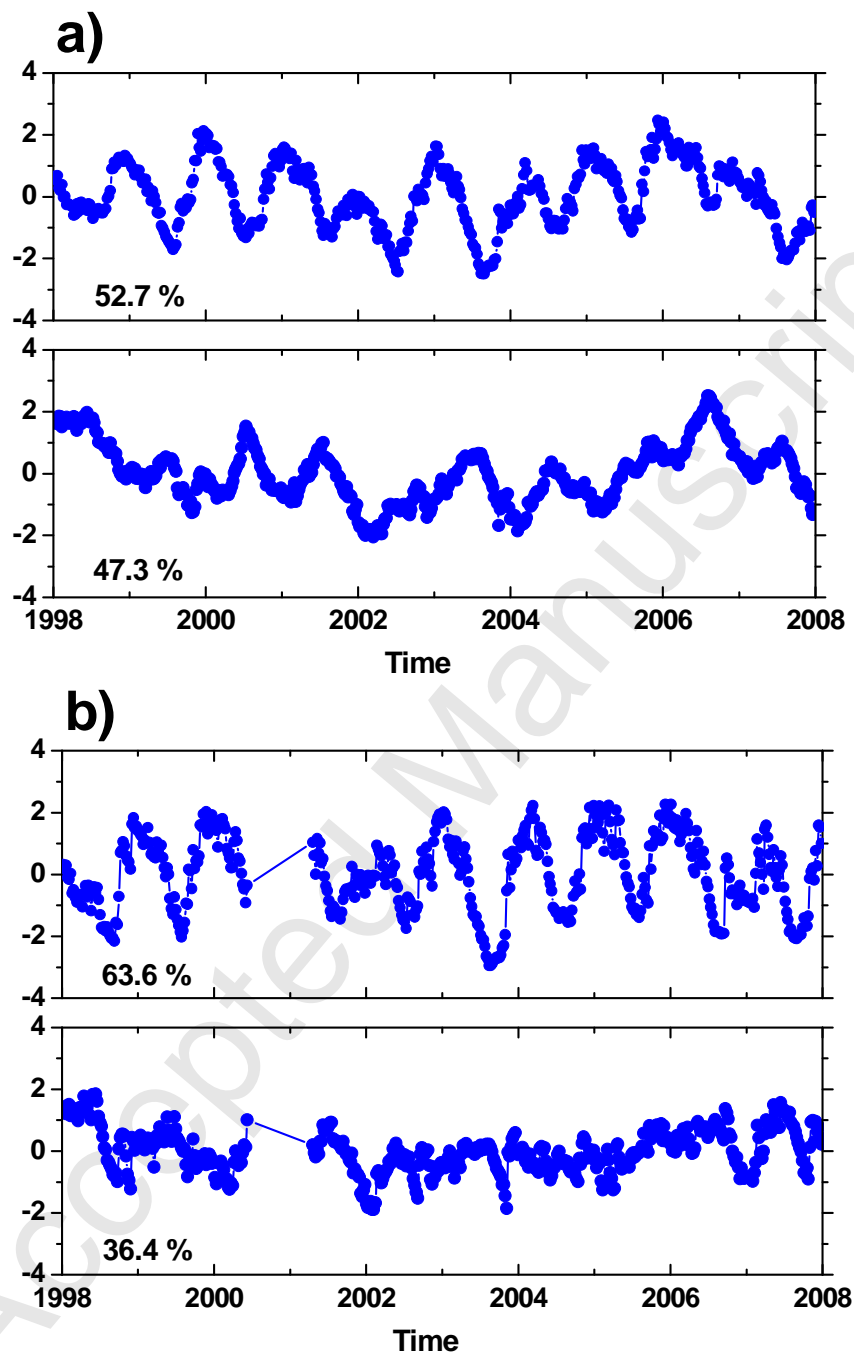


Figure 10

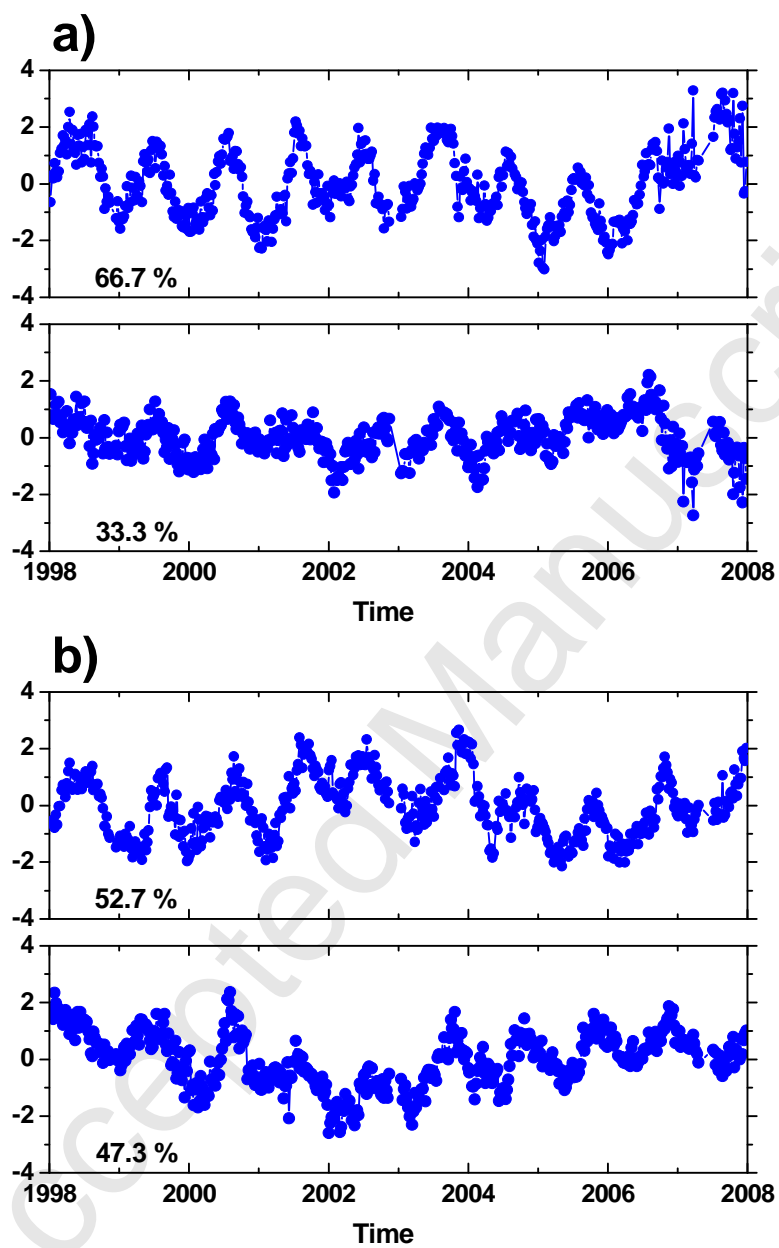


Figure 11

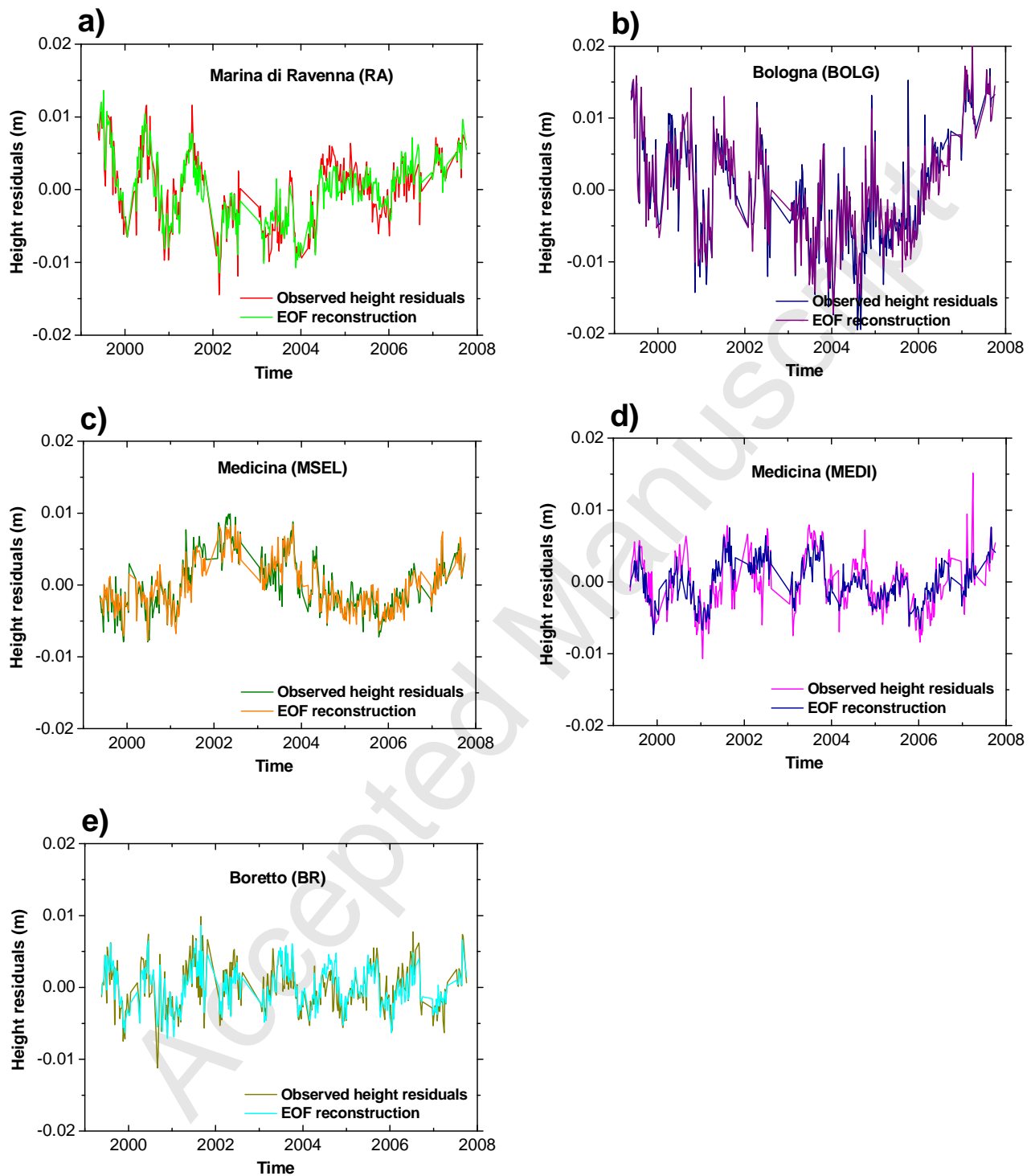


Figure 12

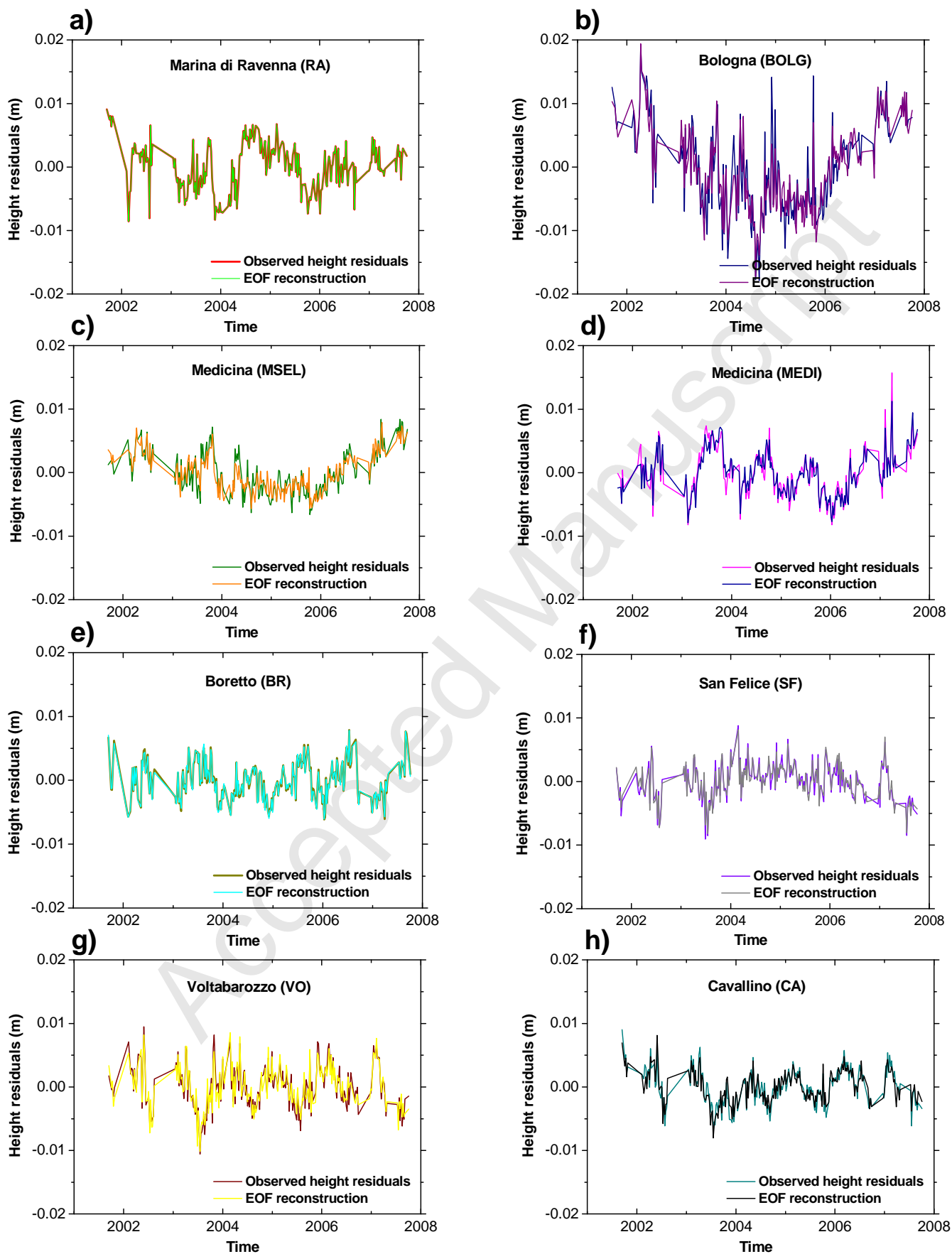


Figure 13

Table 1.

Station name	North/South	Technique	Linear trend
			(mm/yr) GPS (μ Gal/yr) SG, AG
Loiano ^(a) (LOIA)	S	GPS	-1.41 \pm 0.25
		AG	-----
Marina di Ravenna (RA)	S	GPS	-6.51 \pm 0.15
Bologna (BOLG)	S	GPS	-10.57 \pm 0.25
		AG	+4.17 \pm 1.75
		SG	+0.71 \pm 0.05
Medicina (Gravity)	S	AG	+0.52 \pm 0.65
		GPS	-2.44 \pm 0.25
Medicina ^(b) (MEDI)	S	GPS	-2.44 \pm 0.25
Medicina (MSEL)	S	GPS	-2.13 \pm 0.10
Boretto (BR)	S	GPS	-5.00 \pm 0.10
San Felice (SF)	N	GPS	-2.24 \pm 0.15
		GPS	+0.36 \pm 0.15
Votabarozzo (VO)	N	AG	-0.98 \pm 1.07
		GPS	-0.88 \pm 0.40
Marghera (MA)	N	AG	-0.88 \pm 1.41
		GPS	-1.97 \pm 0.15
Cavallino (CA)	N	AG	+0.29 \pm 1.46
		GPS	0.00 \pm 0.25
Treviso (TV)	N	AG	-1.64 \pm 1.50

Table 10

(a)

EOF	PVE	MEDI	SG
1	66.7	+0.71	-0.71
2	33.3	-0.71	-0.71

(b)

EOF	PVE	MSEL	SG
1	52.7	+0.71	-0.71
2	47.3	-0.71	-0.71

Accepted Manuscript

Table 2

EOF	PVE	GPS spatial pattern				
		MSEL	MEDI	RA	BOLG	BR
1	28.1	+0.38	+0.50	+0.43	+0.44	+0.47
2	22.9	-0.62	-0.29	+0.62	+0.37	-0.10
3	19.2	+0.36	-0.08	-0.17	+0.64	-0.65
4	17.1	-0.25	+0.76	+0.16	-0.25	-0.52
5	12.6	-0.53	+0.29	-0.61	+0.44	+0.27

Accepted Manuscript

Table 3

EOF	PVE	GPS spatial pattern							
		MSEL	MEDI	RA	BOLG	BR	CA	SF	VO
1	22.4	+0.12	+0.41	+0.03	-0.13	+0.22	-0.47	-0.48	-0.54
2	19.1	-0.60	-0.26	-0.26	-0.59	-0.24	-0.26	+0.07	-0.13
3	14.5	+0.22	+0.08	-0.70	+0.30	-0.53	-0.19	-0.18	+0.10
4	11.8	+0.01	+0.14	+0.62	-0.01	-0.76	-0.08	-0.07	-0.03
5	11.1	-0.05	-0.66	+0.06	+0.20	-0.03	+0.26	-0.62	-0.25
6	8.2	-0.66	+0.50	-0.09	+0.31	-0.02	+0.42	-0.18	-0.07
7	6.9	+0.36	+0.20	-0.18	-0.57	-0.15	+0.64	-0.10	-0.18
8	5.9	-0.04	+0.12	+0.07	-0.27	+0.11	-0.09	-0.55	+0.76

Accepted Manuscript

Table 4

EOF	PVE	Precipitation spatial pattern			
		ME	RA	BO	BR
1	52.6	+0.55	+0.50	+0.49	+0.46
2	25.1	-0.29	+0.38	-0.63	+0.61
3	15.9	+0.07	-0.77	+0.11	+0.62
4	6.5	-0.78	+0.14	+0.59	+0.15

Accepted Manuscript

Table 5

EOF	PVE	Precipitation spatial pattern						
		ME	RA	BO	BR	CA	SF	VO
1	47.4	+0.40	+0.36	+0.37	+0.41	+0.32	+0.39	+0.39
2	16.1	-0.30	+0.09	-0.50	+0.03	+0.78	-0.13	+0.16
3	13.1	+0.21	+0.79	-0.04	-0.10	0.00	-0.35	-0.45
4	7.6	-0.07	+0.33	-0.45	-0.41	-0.26	+0.65	+0.18
5	6.3	0.00	-0.19	+0.14	-0.02	+0.35	+0.52	-0.74
6	5.8	-0.05	+0.01	+0.52	-0.78	+0.29	-0.08	+0.19
7	3.7	+0.84	-0.31	-0.35	-0.23	+0.12	-0.10	+0.01

Table 6

(a)

SVD	SCP	GPS spatial pattern				
		MSEL	MEDI	RA	BOLG	BR
1	81.3	-0.64	-0.72	-0.01	+0.05	-0.27
2	17.8	+0.24	-0.21	-0.59	-0.73	-0.11
3	0.8	-0.72	+0.52	-0.05	-0.38	+0.24
4	0.0	-0.13	+0.31	-0.68	+0.48	-0.43

(b)

SVD	SCP	Precipitation spatial pattern			
		ME	RA	BO	BR
1	81.3	+0.59	+0.46	+0.56	+0.36
2	17.8	-0.26	+0.64	-0.56	+0.47
3	0.8	+0.23	+0.53	-0.17	-0.80
4	0.0	-0.73	+0.32	+0.59	-0.13

Table 7

(a)

SVD	SCP	GPS spatial pattern							
		MSEL	MEDI	RA	BOLG	BR	CA	SF	VO
1	92.0	-0.55	-0.59	-0.13	-0.19	-0.20	+0.34	+0.25	+0.28
2	6.3	-0.36	+0.23	+0.20	-0.62	-0.19	-0.52	+0.19	-0.23
3	1.3	+0.03	+0.05	-0.95	-0.18	+0.16	-0.16	+0.02	-0.08
4	0.2	+0.03	-0.36	-0.08	+0.40	-0.45	-0.67	-0.16	+0.16
5	0.1	-0.64	+0.17	-0.07	+0.35	-0.02	+0.11	-0.45	-0.46
6	0.1	+0.20	+0.27	-0.15	+0.09	-0.77	+0.32	+0.29	-0.26
7	0.0	+0.25	-0.59	+0.07	-0.04	+0.14	-0.02	+0.14	-0.74

(b)

SVD	SCP	Precipitation spatial pattern						
		ME	RA	BO	BR	CA	SF	VO
1	92.0	+0.39	+0.39	+0.38	+0.37	+0.39	+0.39	+0.33
2	6.3	-0.22	+0.24	-0.50	-0.19	+0.76	-0.16	+0.06
3	1.3	+0.24	+0.58	+0.29	-0.45	-0.15	-0.54	+0.01
4	0.2	-0.46	-0.35	+0.54	-0.23	+0.21	-0.14	+0.51
5	0.1	+0.45	-0.36	-0.16	+0.39	+0.09	-0.63	+0.29
6	0.1	-0.13	-0.06	+0.44	+0.30	+0.35	-0.27	-0.71
7	0.0	-0.56	+0.43	-0.09	+0.57	-0.28	-0.22	+0.20

Table 8

(a)

EOF	PVE	MEDI	WT
1	62.3	+0.71	-0.71
2	37.7	+0.71	+0.71

(b)

EOF	PVE	MSEL	WT
1	59.9	+0.71	-0.71
2	40.1	+0.71	+0.71

Accepted Manuscript

Table 9

(a)

EOF	PVE	Prec.	SG
1	52.7	+0.71	+0.71
2	47.3	+0.71	-0.71

(b)

EOF	PVE	WT	SG
1	63.6	+0.71	+0.71
2	36.4	+0.71	-0.71

Accepted Manuscript